



COMPUTATIONAL FLUID DYNAMIC MODEL FOR THE FULLY-DEVELOPED  
LAMINAR FLOW IN A VERTICAL COLUMN WITH DIFFERENT  
FEED INLET DESIGNS

MR. POOCHET HORKANYA

A SPECIAL RESEARCH PROJECT SUBMITTED IN PARTIAL FULFILLMENT  
OF THE REQUIREMENTS FOR  
THE DEGREE OF MASTER OF ENGINEERING (CHEMICAL ENGINEERING)  
FACULTY OF ENGINEERING  
KING MONGKUT'S UNIVERSITY OF TECHNOLOGY THONBURI

2011

Computational Fluid Dynamic Model for the Fully-developed Laminar Flow in a Vertical  
Column with Different Feed Inlet Designs

Mr. Poochet Horkanya B.Eng. (Chemical Engineering)

A Special Research Project Submitted in Partial Fulfillment  
of the Requirements for  
The Degree of Master of Engineering (Chemical Engineering)  
Faculty of Engineering  
King Mongkut's University of Technology Thonburi  
2011

Special Research Project Committee

.....  
(Asst. Prof. Veera Loha, Ph.D.) Chairman of Special Research  
Project Committee

.....  
(Assoc. Prof. Thongchai Srinophakun, Ph.D.) Member and Special  
Research Project Advisor

.....  
(Asst. Prof. Kwanchanok Pasuwat, Ph.D.) Member of Special  
Research Project Committee

Copyright reserved

Special Research Project Title	Computational Fluid Dynamic Model for the Fully-developed Laminar Flow in a Vertical Column with Different Feed Inlet Designs
Special Research Project Credits	6
Candidate	Mr. Poochet Horkanya
Special Research Project Advisor	Assoc. Prof. Dr. Thongchai Srinophakun
Program	Master of Engineering
Field of Study	Chemical Engineering
Department	Chemical Engineering
Faculty	Engineering
B.E.	2554

### Abstract

As well understood for a development of crystallizer, it is important that the laminar flow profile established as quickly as possible after the fluid enters. Three feed inlets; 16-pipes inlet, one pipe upward inlet and one pipe sideward inlet, have been equipped to achieve this purpose. The objective of thesis is therefore to model the fluid flow in the vertical column using CFD techniques in order to explain the inlet types, which provide the laminar flow profile at the lowest position of the column. Firstly, the supplementary data including the dimensions of a vertical column and feed inlets are gathered in order to create the geometry and to generate the volume elements in the pre-process step. The basic and indispensable governing equations of fluid motion are the equation of continuity and the Navier-Stokes equations. The simulation results are analyzed to demonstrate the velocity profile and streamlines. It was found that 16-pipes inlet can provide the fully-developed laminar flow fastest at 7 cm from the inlet level followed by one pipe sideward inlet at 10 cm and one pipe upward inlet at 11 cm. Moreover, the new design of pipe inlet is proposed in order to improve the distribution of the liquid feed. The simulation result shows the proposed feed inlet can develop the laminar flow fastest at 6 cm from reference level.

In addition, a set of experiments is performed to verify these CFD models. Dye was used to observe the fluid flow behavior at the steady-state condition. The comparison between the pathway of dye from the experiments and the streamline from CFD simulation are discussed in this thesis.

**Keywords:** Fully developed laminar flow / Vertical column / Feed inlet design / Velocity profile / CFD model

หัวข้อโครงการศึกษาวิจัย	แบบจำลองการคำนวณทางพลศาสตร์ของไหลสำหรับการไหลแบบลามินาร์สมบูรณ์ในท่อแนวตั้งที่มีการออกแบบทางป้อนเข้าต่างกัน
หน่วยกิต	6
ผู้เขียน	นายภูษิษฐ์ หอกันยา
อาจารย์ที่ปรึกษา	รศ.ดร. ชงไชย ศรีนพคุณ
หลักสูตร	วิศวกรรมศาสตรมหาบัณฑิต
สาขาวิชา	วิศวกรรมเคมี
ภาควิชา	วิศวกรรมเคมี
คณะ	วิศวกรรมศาสตร์
พ.ศ.	2554

### บทคัดย่อ

ตามที่เข้าใจกันอย่างแพร่หลายเกี่ยวกับการพัฒนาเครื่องตกผลึกว่าของไหลจะต้องมีการไหลเป็นแบบลามินาร์เร็วที่สุดเท่าที่จะทำได้หลังจากที่ของไหลถูกป้อนเข้าสู่เครื่องตกผลึก ทางเข้า 3 แบบ อันได้แก่ ทางเข้าแบบ 16 ท่อทิศขึ้นด้านบน, ทางเข้าแบบท่อเดียวทิศขึ้นด้านบนและทางเข้าแบบท่อเดียวทิศไปด้านข้าง จึงถูกออกแบบมาให้บริการความต้องการข้างต้น ดังนั้นวัตถุประสงค์ของวิทยานิพนธ์ฉบับนี้จึงเป็นการจำลองการไหลของของไหลในท่อแนวตั้งโดยใช้เทคนิคการคำนวณทางพลศาสตร์ของไหล เพื่อหาว่าทางเข้าแบบใดให้โปรไฟล์ความเร็วเป็นแบบลามินาร์สมบูรณ์ที่ระดับความสูงต่ำที่สุด เริ่มแรกข้อมูลที่สำคัญ เช่น ขนาดของท่อแนวตั้งและทางเข้าทั้ง 3 ชนิด จะถูกรวบรวมเพื่อใช้ในการสร้างปริมาตรควบคุมของแบบจำลองและแบ่งออกเป็นปริมาตรเล็กๆในการคำนวณ สมการพื้นฐานแต่ขาดไม่ได้ที่ใช้ในการอธิบายการเคลื่อนที่ของของไหลคือสมการความต่อเนื่องและสมการนิเวียร์-สโต็ค ผลการคำนวณจะถูกวิเคราะห์และแสดงออกมาในรูปโปรไฟล์ความเร็วและเส้นทางการไหล พบว่าทางเข้าแบบ 16 ท่อทิศขึ้นด้านบนให้การไหลเป็นแบบลามินาร์สมบูรณ์เร็วที่สุดที่ระยะ 7 เซนติเมตร วัดจากทางเข้า รองลงมาคือทางเข้าแบบท่อเดียวทิศไปด้านข้างให้การไหลเป็นแบบลามินาร์สมบูรณ์ที่ระยะ 10 เซนติเมตรและสุดท้ายคือทางเข้าแบบท่อเดียวทิศขึ้นด้านบนที่ระยะ 11 เซนติเมตร นอกจากนี้ยังมีการออกแบบทางเข้าแบบใหม่เพื่อทำให้มีการกระจายตัวของของเหลวที่ป้อน ผลการคำนวณแสดงให้เห็นว่าทางเข้าแบบใหม่ให้การไหลเป็นแบบลามินาร์สมบูรณ์ที่ระยะ 6 เซนติเมตรและเร็วที่สุด

รวมทั้งการทดลองได้ถูกจัดทำขึ้นเพื่อใช้ตรวจสอบความถูกต้องของแบบจำลอง ลีข้อมถูกใช้ในการสังเกตพฤติกรรมของการไหลของของไหลที่สภาวะคงตัว ซึ่งการเปรียบเทียบระหว่างเส้นทางการไหลของลีข้อมจาก

การทดลองและเส้นทางการไหลของสีย้อมจากการจำลองได้ถูกอธิบายไว้ในวิทยานิพนธ์ฉบับนี้

คำสำคัญ: การไหลแบบลามินาร์สมบูรณ์ / หอแนวตั้ง / การออกแบบทางป้อนเข้า / โปรไฟล์ความเร็ว  
แบบจำลองการคำนวณทางพลศาสตร์ของไหล

## **ACKNOWLEDGEMENTS**

This project cannot be accomplished without direct and indirect assistance from many people. Foremost, the author would like to express his gratitude to the advisor of this project, Assoc. Prof. Thongchai Srinophakun for all technical support and valuable guidance. The author also appreciates the supervisor, Prof. Anthony Paterson of Massey University for suggestions about this project and his kindly support during oversea study. In addition, the author would like to thank to Asst. Prof. Veera Loha and Asst. Prof. Kwanchanok Pasuwat, project committees, for attention to this research project and their valuable ideas to improve the work.

Moreover, the author would like particularly express special thanks to the staff of Chemical Engineering Practice School (ChEPS), Mrs. Chadaporn Dammunee, who helped the author with communication and any important information used to finish the master's degree. Lastly, this project would not have been completed without lots of support from the author's family and friends.

## CONTENTS

	PAGE
ENGLISH ABSTRACT	ii
THAI ABSTRACT	iii
ACKNOWLEDGEMENTS	v
CONTENTS	vi
LIST OF TABLES	viii
LIST OF FIGURES	ix
 <b>CHAPTER</b>	
<b>1. INTRODUCTION</b>	<b>1</b>
1.1 Background	1
1.2 Objectives	2
1.3 Scopes of work	2
 <b>2. THEORY AND LITERATURE REVIEWS</b>	<b>3</b>
2.1 Crystallization	3
2.2 Finite Element Method	7
2.3 Computational Fluid Dynamics	9
2.4 Literature reviews	11
2.4.1 Uniformity of particles from laminar jet break-up	11
2.4.2 Nucleation of Alpha lactose monohydrate induced using flow through a venturi orifice	15
2.4.3 Fully-Developed Flow in a Pipe: A CFD Solution	17
 <b>3. METHODOLOGY</b>	<b>21</b>
3.1 ANSYS FLUENT software	21
3.2 Input data preparation	21
3.3 Creation of CFD models	21
3.4 Analysis and interpretation of CFD simulation results	22
3.5 Validation of the simulation results with experimental data	23
 <b>4. RESULTS AND DISCUSSION</b>	<b>24</b>
4.1 16-pipes inlet	25
4.1.1 The effect of the number of meshes on the simulation results	25
4.1.2 Development of the geometry of a vertical column	26
4.1.3 The velocity profiles of a fluid at various heights of a vertical column	27
4.2 One pipe upward inlet	31
4.2.1 The effect of the number of meshes on the simulation results	31

4.2.2 The velocity profiles of a fluid near fully-developed laminar flow	32
4.3 One pipe upward inlet	33
4.3.1 The effect of the number of meshes on the simulation results	33
4.3.2 The velocity profiles of a fluid near fully-developed laminar flow	34
4.4 All feed inlets	35
4.4.1 Comparison of the type of inlet developing the laminar flow at the lowest position	35
4.4.2 Validation of CFD models with experimental data	36
4.5 New one pipe inlet	45
4.5.1 Comparison between the 16-pipes upward inlet and the new one pipe inlet	46
<b>5. CONCLUSION AND RECOMMENDATION</b>	<b>47</b>
5.1 Conclusion	47
5.2 Suggestions	47
5.3 Future works	47
<b>REFERENCES</b>	<b>48</b>
<b>APPENDIX</b>	<b>49</b>
A. The geometry of crystallization column and feed inlets	49
B. The physical properties	54
C. Experimental data	56
<b>CURRICULUM VITAE</b>	<b>70</b>



## LIST OF TABLES

<b>TABLE</b>	<b>PAGE</b>
2.1 Artificial Method for Crystallization	6
2.2 The Comparison between Experiments and Simulation Aspects	10
2.3 The Characteristics of Experiments and Simulation	10
B.1 The physical properties of material	55
C.1 represents the velocity of dye in each nozzle at different levels of height	68

## LIST OF FIGURES

FIGURE	PAGE
2.1 Table Salt (Sodium Chloride)	3
2.2 Crystallization Process	4
2.3 Snow flake	5
2.4 FEM of a complex system	8
2.5 Flooding situation in Bangkok, Thailand 2011	9
2.6 Effect of jet velocity on particle size distribution	12
2.7 Relationship between nozzle size and particle size	13
2.8 Effect of nozzle diameter on particle size distribution	13
2.9 Effect of PLC concentration on jet phase viscosity	14
2.10 Effect of jet phase viscosity on particle size distribution	15
2.11 Comparison of the Venturi orifice diameter on the number of crystals per ml at different Reynolds numbers (log scale)	16
2.12 Comparison of the Venturi orifice diameter on the number of crystals per ml at different Reynolds numbers (linear scale)	17
2.13 Geometry of a fully-developed flow in a pipe	18
3.1 The project schematic of ANSYS Workbench	22
3.2 Methodology	23
4.1 The velocity profiles of fluid at the bottom of the column using different in spatial discretization and the number of meshes	25
4.2 The velocity profiles of fluid at the bottom of the column with and without a cone shape	26
4.3 The velocity profiles of fluid at the position below a feed inlet	27
4.4 The velocity profiles of fluid at the position of a feed inlet	28
4.5 The velocity profiles of fluid at the position above a feed inlet	29
4.6 The velocity profiles of fluid at the position near a fully-developed laminar flow	30
4.7 The velocity profiles of fluid at the bottom of the column using different in spatial discretization and the number of meshes	31
4.8 The velocity profiles of fluid at the position near a fully-developed laminar flow	32
4.9 The velocity profiles of fluid at the bottom of the column using different in spatial discretization and the number of meshes	33
4.10 The velocity profiles of fluid at the position near a fully-developed laminar flow	34
4.11 The comparison of heights in which feed inlet designs develop the fully-developed laminar flow	35
4.12 The streamlines of fluid of a vertical column with 16-pipes inlet	38
4.13 The streamlines of fluid of a vertical column with one pipe upward inlet	41
4.14 The streamlines of fluid of a vertical column with one pipe sideward inlet	44

4.15 New one pipe inlet	45
4.16 The velocity profiles of fluid at the position near a fully-developed laminar flow	45
4.17 The comparison of heights in which feed inlet designs develop the fully-developed laminar flow	46
A.1 The crystallization of the column	50
A.2 The reference level of CFD models	51
A.3 The dimensions of 16-pipes inlet type	52
A.4 The dimensions of one pipe upward inlet type	52
A.5 The dimensions of one pipe side inlet type	53
A.6 The dimensions of one pipe side inlet type	53
C.1 16-pipes inlet at the initial time, $t = 0$ (16sec dye injected)	58
C.2 16-pipes inlet at time, $t = 14$ seconds (30 sec dye injected)	58
C.3 16-pipes inlet at time, $t = 34$ seconds (50 sec dye injected)	59
C.4 16-pipes inlet at time, $t = 5$ minutes 22 seconds (6mins 29sec dye injected)	59
C.5 16-pipes inlet at time, $t = 4$ minutes 58 seconds (7mins 5sec dye injected)	60
C.6 16-pipes inlet at 39 cm height	60
C.7 One pipe upward inlet near the initial time of injection (31sec dye injected)	61
C.8 One pipe upward inlet at the time, $t = 14$ seconds (45sec dye injected)	61
C.9 One pipe upward inlet at the time, $t = 43$ seconds (1min14sec dye injected)	62
C.10 One pipe upward inlet at the time, $t = 1$ minutes 30 seconds (2min dye injected)	62
C.11 One pipe upward inlet at the time, $t = 14$ seconds (42sec dye injected)	63
C.12 One pipe upward inlet at the time, $t = 28$ seconds (58sec dye injected)	63
C.13 One pipe upward inlet at the time, $t = 1$ minutes 50 seconds (2min 17sec dye injected)	64
C.14 One pipe upward inlet at the time, $t = 5$ minutes 20 seconds (5min 47sec dye injected)	64
C.15 One pipe sideward inlet near the initial time of injection (39sec dye injected)	65
C.16 One pipe sideward inlet at the time, $t = 10$ seconds (50sec dye injected)	65
C.17 One pipe sideward inlet at the time, $t = 67$ seconds (1min 46sec dye injected)	66
C.18 One pipe sideward inlet at the time, $t = 1$ minute 30 seconds (2min 10sec dye injected)	66
C.19 One pipe sideward inlet at the time, $t = 1$ minute 30 seconds (11min 4sec dye injected)	67
C.20 One pipe sideward inlet at the time, $t = 3$ minutes 40 seconds (12min 47sec dye injected)	67
C.21 One pipe sideward inlet at the time, $t = 6$ minutes 52 seconds (15min 58sec dye injected)	68

# CHAPTER 1 INTRODUCTION

## 1.1 Background

Computational fluid dynamics (CFD) is a simulation tool, which uses governing equations and numerical methods to solve and analyze the fluid flow patterns for pre-defined geometries and boundary conditions. The basic governing equations of fluid motion called the Navier-Stokes equations have been known more than one hundred years. A high-performance computer also plays a major role in the time consumption and the accuracy of results.

The advantages of CFD are time and cost saving, capability of visualization, experimental validation, designing for optimization and performance prediction. The simulation allows checking the designs and concepts without spending money or effort to build actual equipment. In some cases, an experiment is almost impossible or too expensive to perform such as satellite launching, aircraft aerodynamics and weather forecast etc. the simulation would be suitable for them.

In the past ten years, CFD has been applied dramatically observed from many journals and researches relevant. The commercial programs are available and released continuously such as COMSOL, ANSYS CFX, FLUENT and XFLOW etc. Today, this technology has widely been applied to engineering design such as automobile and aircraft, civil engineering, weather science and oceanography.

Nowadays, a laminar flow crystallizer is being developed by Massey University, New Zealand. According to a previous literature that name is Uniformity of particles from laminar jet break-up. It is important that the laminar flow profile established as quickly as possible in order to get crystals with low size distribution. The laminar jet break-up is one of the easiest methods to produce the uniform particles in a crystallization process. Thus, three inlets were designed to rapidly develop the laminar flow and were made to be used in the experiment. This study is to model the fluid flow in the column using CFD techniques of different feed inlet designs and find out which one can develop the laminar flow profile at the lowest position. The velocity profiles of fluid in the region around the inlet are also interest and will be expressed by this technique.

## **1.2 Objective**

- 1 To present which feed inlets can develop the laminar flow at the lowest position of a vertical column.
- 2 To simulate the fluid flow within a vertical column for each feed inlet design and validate with the experimental data.
- 3 To demonstrate the velocity profiles across a vertical column at distance around the feed inlet.
- 4 To propose the new feed inlet design for a fully-developed laminar flow.

## **1.3 Scope of work**

1. The input data for a CFD simulation including the geometry of the column, the dimension of various inlets and the property of material etc., is collected from Technology and Science, Massey University, New Zealand.
2. The CFD models for prediction the fluid flow in 3.5 meter height vertical column with three different feed inlets are created by using the FLUENT software.
3. Experiments and record data are performed in laboratory at Massey University in order to check with the simulation result.

## CHAPTER 2 THEORY AND LITERATURE REVIEWS

In chapter 2, the theory and previous literatures related to this thesis are studied. The basic knowledge such as meaning, process and application of crystallization is described in the first section. The second section is the reviews of Finite Element Method. It is an original ideal of computational fluid dynamics.

### 2.1 Crystallization<sup>[1]</sup>

Crystallization is a natural or artificial process of solid crystal formation precipitating from a solution. It is rarely to found crystals, which melt or deposit directly from a gas. Crystallization is also a chemical solid–liquid separation technique, in which mass transfer of a solute from the liquid solution to a pure solid crystalline phase occurs. In chemical engineering, crystallization occurs in a crystallizer. Crystallization is therefore an aspect of precipitation, obtained through a variation of the solubility conditions of the solute in the solvent.



**Figure 2.1** Table Salt (Sodium Chloride)

(Source:<http://www.art.com/products/p360921795-sa-i4011972/bill-beatty-table-salt-crystals-sodium-chloride.htm>, 2011)

Figure 2.1 shows an example of solid crystals. Crystals of the same substance form a similar structure in nature, but there are many basic crystalline structures in different substances

### Crystallization process

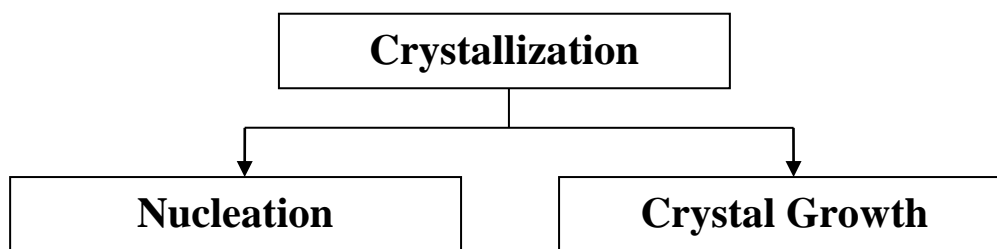


**Figure 2.2** Crystallization Process

The crystallization process consists of two major steps, nucleation and crystal growth, as Figure 2.2. Nucleation is the step where the solute molecules dispersed in the solvent start to gather into clusters on the nanometer scale. The concentration of solute elevates in a small region, which become stable under the current operating conditions. These stable clusters constitute the nuclei. However, when the clusters are not stable, they redissolve. Therefore, the clusters need to reach a critical size in order to become stable nuclei. Such critical size is dictated by the operating conditions such as temperature, concentration and supersaturation etc. It is at the stage of nucleation that the atoms arrange in a defined and periodic manner that defines the crystal structure — note that "crystal structure" is a special term that refers to the relative arrangement of the atoms, not the macroscopic properties of the crystal like size and shape, although those are a result of the internal crystal structure.

The crystal growth is the subsequent growth of the nuclei that succeed in achieving the critical cluster size. Nucleation and growth continue to occur simultaneously while the supersaturation exists. Supersaturation is the driving force of the crystallization; hence, the rate of nucleation and growth is driven by the existing supersaturation in the solution. Depending upon the conditions, either nucleation or growth may be predominant over the other, and as a result, crystals with different sizes and shapes are obtained. To control the crystal size and shape, it is the main challenges in industrial manufacturing for pharmaceuticals. Once the supersaturation is exhausted, the solid–liquid system reaches equilibrium and the crystallization is complete, unless the operating conditions are modified from equilibrium to supersaturate the solution again.

## Polymorphism

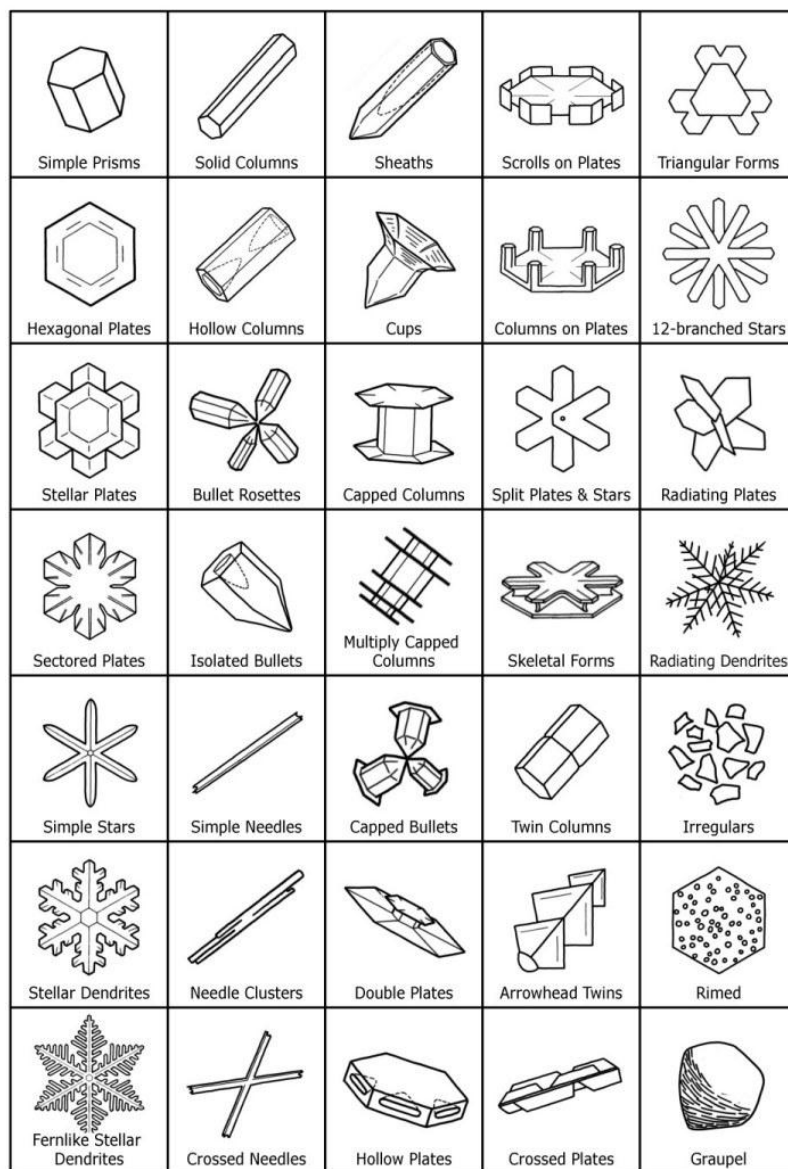


**Figure 2.3** Snow flake

(Source: <http://www.cco.caltech.edu/~atomic/snowcrystals/class/class.htm>, 1954)

Many compounds have the ability to crystallize with different crystal structures, a phenomenon called polymorphism. Each polymorph is in fact a different thermodynamic solid state and crystal polymorphs of the same compound exhibit different physical properties, such as dissolution rate, shape (angles between facets and facet growth rates), melting point, etc. For this reason, polymorphism is of major importance in industrial manufacture of crystalline products. The snow crystals also have many crystal polymorphs as shown in Figure 2.3.



### Nature crystallization

For nature crystallization, there are many examples of natural process that involve crystallization. Geological time scale process include: (1) Natural (mineral) crystal formation such as gemstone and (2) Stalactite/stalagmite, rings formation. Usual time scale process include: (1) Snowflakes formation (Koch snowflake) and (2) Honey crystallization (nearly all types of honey crystallize).

### Artificial method <sup>[2]</sup>

For crystallization, a solution must be supersaturated to ignite the process. This means that the solution has to contain more solute (molecules or ions) dissolved than it would contain under the equilibrium or saturated solution. This can be achieved by various methods as following table.

**Table 2.1** Artificial Method for Crystallization

Mode	Method
Cooling	Reduction in temperature
Dilution	Addition anti-solvent
Reaction	Generation of solute
Evaporation	Loss of solvent
Precipitation	Changing pH of solution

There are many artificial methods for crystallization such as solution cooling, addition of a second solvent to reduce the solubility of the solute known as anti-solvent, chemical reaction and changing pH which is the most common methods used in industrial practice.

Other methods, such as solvent evaporation, can also be used. The spherical crystallization has some advantages (flow ability and bioavailability) for the formulation of pharmaceutical drugs

### Applications

There are two major groups of applications for the artificial crystallization process which are crystal production and purification.

### Crystal production

From a material industry perspective, a macroscopic crystal production supplies the demand of natural-like crystals with methods that "accelerate time-scale" for massive production and/or perfection;(1) Ionic crystal production and (2) Covalent crystal production.

Tiny size crystals such as powder, sand and smaller sizes, are produced by methods for powder and controlled (nanotechnology fruits) forms. Salt-powder production is one of mass-production on chemical industry. For massive production examples are powder salt for food industry, silicon crystal wafer production and production of sucrose from sugar beet, where the sucrose is crystallized out from an aqueous solution.

On the other hand, Small production of tiny crystals for sample production is focused on material characterization. Controlled recrystallization is an important method to supply unusual crystals, which need to reveal the molecular structure and nuclear forces inside a typical molecule of a crystal. Many techniques, like crystallography, X-ray and NMR spectroscopy, are widely used in chemistry and biochemistry to determine the structures of an immense variety of molecules, including inorganic compounds and biomacromolecules.

### **Purification**

Crystallization is used to improve and/or verify their purity to obtain very pure substance. It can separate a product from a liquid feed stream, often in extremely pure form, by cooling the feed stream or adding precipitants, which lower the solubility of the desired product so that it forms crystals.

Well-formed crystals are expected to be pure because each molecule or ion must fit perfectly into the lattice as it leaves the solution. Impurities would normally not fit as well in the lattice, and thus remain in solution preferentially. Hence, molecular recognition is the principle of purification in crystallization. However, there are instances when impurities incorporate into the lattice, hence, decreasing the purity of the final crystal product. Also, in some cases, the solvent may incorporate into the lattice forming a solvate. In addition, the solvent may be 'trapped' (in liquid state) within the crystal formed, and this phenomenon is known as inclusion.

## **2.2 Finite Element Method <sup>[3]</sup>**

One of the numerical techniques for finding approximate solutions of partial differential equations (PDE) is the finite element method (FEM) or finite element analysis (FEA). This method is a good choice for solving partial differential equations over complicated domains such as when the domain changes (as during a solid-state reaction with a moving boundary), when the desired precision varies over the entire domain, or when the solution lacks smoothness. The solution approach is based either on eliminating the differential equation completely (steady state problems), or rendering the PDE into an approximating system of ordinary differential equations, which are then numerically integrated using standard techniques such as Euler's method, Runge-Kutta, etc. In this technique, an approximate numerical solution is obtained by satisfying the conditions of the

differential equations (equilibrium, continuity, etc.) at discrete points. The accuracy being improved by successive refinement of the size of the contributing domains and the consequent increase in the points at which the field conditions are satisfied. In setting up the nodal equations for approximation of the differential equations, a variety of techniques can be used. In solving partial differential equations, the primary challenge is to create an equation that approximates the equation to be studied, but is numerically stable, meaning that errors in the input and intermediate calculations do not accumulate and cause the resulting output to be meaningless.

FEM software provides a wide range of simulation options for controlling the complexity of both modeling and analysis of a system. FEM consists of a computer model of a material or design to analyze specific results. It is used in the new product design, and the existing product refinement. A company is able to verify a proposed design will be able to perform to the client's specifications prior to manufacturing or construction. Modifying an existing product or structure is utilized to qualify the product or structure for a new service condition.

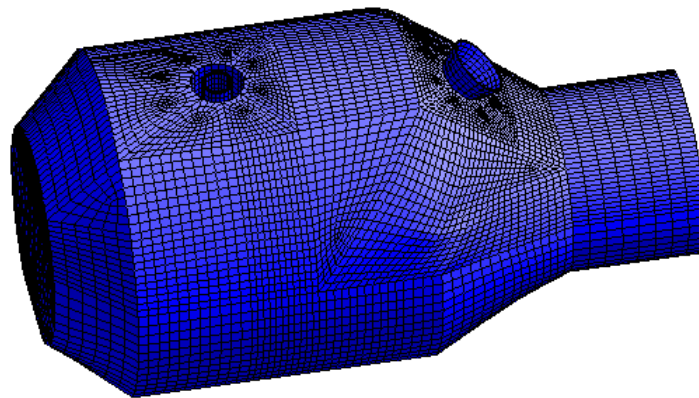


**Figure 2.4** FEM of a complex system

(Source: [http://cse.gre.ac.uk/coursinf/cfd\\_exp.html](http://cse.gre.ac.uk/coursinf/cfd_exp.html))

FEM uses a complex system of points called nodes which make a grid called a mesh as shown in Figure 2.4. Nodes are assigned at a certain density throughout the material depending on the anticipated stress levels of a particular area. Regions, which will receive large amounts of stress usually, have a higher node density than those, which experience little or no stress. The mesh acts like a spider web in that from each node, there extends a mesh element to each of the adjacent nodes. This web of vectors is what carries the material properties to the object, creating many elements. There are generally two types of analysis, which are 2-D modeling and 3-D modeling used in industry. 3-D modeling produces results that are more accurate.

## 2.3 Computational Fluid Dynamics <sup>[4]</sup>

Computational Fluid Dynamics (CFD) is a simulation tool, which uses powerful computers in combination with numerical methods and governing equations to solve and analyze fluid flow situations. It provides a qualitative and sometimes quantitative prediction of fluid flow and enables scientists and engineering to perform numerical experiments for visualization.

### Application

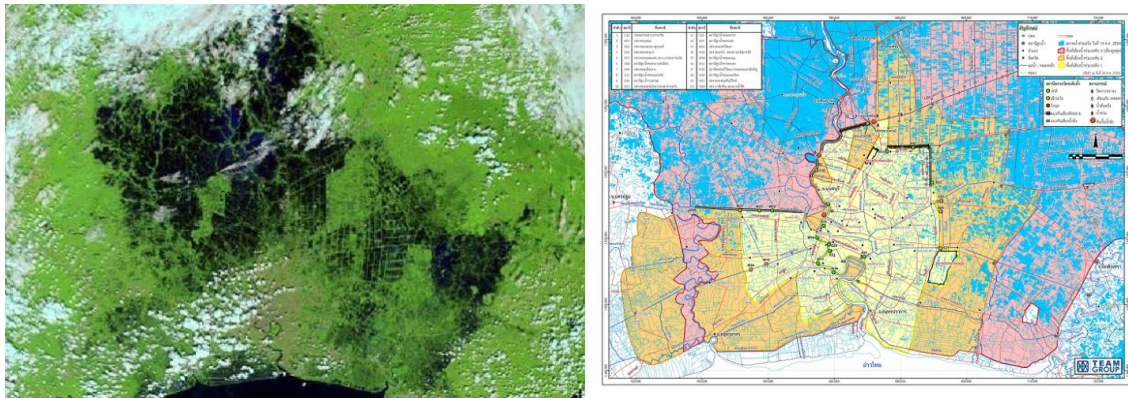


**Figure 2.5** Flooding situation in Bangkok, Thailand 2011

(Source: (left) <http://news.sanook.com/gallery/gallery/1068332/245938/>, (right) <http://www.review-trend.com>, 2011)

There are many fluid flow problems encountered in everyday life. For example, meteorological phenomena (rain, wind, hurricanes, floods and fires), environmental hazards (air pollution, transport of contaminants), heating and air conditioning of building or cars, combustion in automobile engines and propulsion systems, interaction of various objects in surrounding air or water, complex flows in furnaces, heat exchangers and chemical reactors, processes in human body (blood flow, breathing and drinking). Figure 2.5 shows the flooding situation in Thailand, which can be modified using a CFD simulation for prediction of the water flow and level.

### Experiments vs. Simulation <sup>[5]</sup>

CFD gives an insight into flow patterns that are difficult, expensive or impossible to study using traditional experimental technique. The comparison between experiment and simulation is shown in the table 2.2.

**Table 2.2** The Comparison between Experiments and Simulation Aspects

Experiments	Simulation
Quantitative description of flow phenomena using measurement <ul style="list-style-type: none"> <li>- for one quantity at a time</li> <li>- at a limited numbers of points and time instants</li> <li>- for a laboratory-scale model</li> <li>- for limited range of problems and operating conditions</li> </ul> <b>Error sources:</b> measurement errors and disturbance by the probes	Quantitative description of flow phenomena using CFD software <ul style="list-style-type: none"> <li>- for all desired quantities</li> <li>- with high resolution in space and time</li> <li>- for the actual flow domain</li> <li>- for virtually any problem and realistic operation conditions</li> </ul> <b>Error sources:</b> modeling, discretization, iteration and implementation

As a rule, CFD does not replace the measurement completely but the amount of experiment and the overall cost can be significantly reduced. While the experiment and personnel are difficult to transport, CFD software is portable and easy to use and modify. The characteristics of experiments and simulation are shown as following.

**Table 2.3** The Characteristics of Experiments and Simulation

Experiment	Simulation
Expensive	Cheaper
Slow	Faster
Sequential	Parallel
Single-purpose	Multiple-purpose

The results of a CFD simulation are one hundred percent never reliable because the input data may involve too many guessing or imprecision and the mathematical model of the problem at hand may be inadequate. Moreover, the accuracy of the results is limited by the available computing power.

### Computational Fluid Dynamics Analysis Process

Firstly, well understand and define of problem statement is necessary to achieve before a CFD simulation will launch. The flow problem according physical phenomena, geometry of a domain and operating conditions need to be identified. A suitable mathematic model and the reference frame are chosen to solve a correct solution.

Secondly, The PDE system is transformed into a set of algebraic equations or so called discretization process. Mesh is generated to separate the domain into cells or elements (triangular or quadrilateral). 1<sup>st</sup> or high order space discretization is defined for approximation of spatial derivatives while time discretization for approximation of temporal derivatives is specified in term of explicit or implicit schemes.

Next, Iterative solution strategy must be used to solve the coupled nonlinear algebraic equations. There are two types of iteration of solution, which are outer and inner iterations. For outer iterations, the coefficients of the discrete problem are updated using the solution values from the previous iteration so as to get rid of the nonlinearities by a Newton method and solve the governing equation in a segregated fashion. The inner iterations are the resulting sequence of linear sub problems typically solved by an iterative method (conjugate gradients) because direct solvers (Gaussian elimination) are prohibitively expensive. Convergence criteria are necessary to check the residuals, relative solution changes and other indicators to make sure that the iterations converge.

The last step is a post-processing. The post-processing of the simulation results is performed in order to extract the desired information from the computational solution. For examples, derived quantities (stream function, vorticity), integral parameters (lift, drag and total mass) and visualization data showing in arrow plot, particle tracking and streamlines.

## **2.4 Literature reviews**

This topic will show the reference literature that relates to this thesis. The specific knowledge about uniformity of particles from laminar jet break up, effect of flow pattern (Reynolds number) to crystallization and a CFD simulation for fully-developed flow in a pipe is studied and collected in this section.

### **2.4.1 Uniformity of particles from laminar jet break-up<sup>[6]</sup>**

This research studies on the relationship between the uniformity of the resultant particles and the operating conditions. Poly- $\epsilon$ -caprolactone (PLC) in which molecular weight equals 65,000 was used to form the solid particles. The particles were made in a batch process by two steps. Firstly, PLC containing in dichloromethane (DCM) was injected into an aqueous solution by a syringe pump with a needle. The aqueous solution consists of polyvinyl alcohol (PVA) as a stabilizer. After the injection completed, the newly formed droplets was gently stirred and heated to allow DCM to evaporate and PCL dissolved in DMC to precipitate out. The oil droplets were converted into spherical solid beads. The particles were filtered out and collected for size measuring by optical microscope.

It is generally knowledge that the solid particle size is determined by properties of materials and process variables. There are only three parameters have been investigated in the literature such as jet velocity, nozzle size and jet phase velocity. The uniformity of particles is measured coefficient of variance (%) as shown below.

$$CV = \frac{\sqrt{\frac{\sum_i^n (d_i - \bar{d})^2}{(n-1)}}}{\bar{d}} \quad (0)$$

### Influence of jet velocity

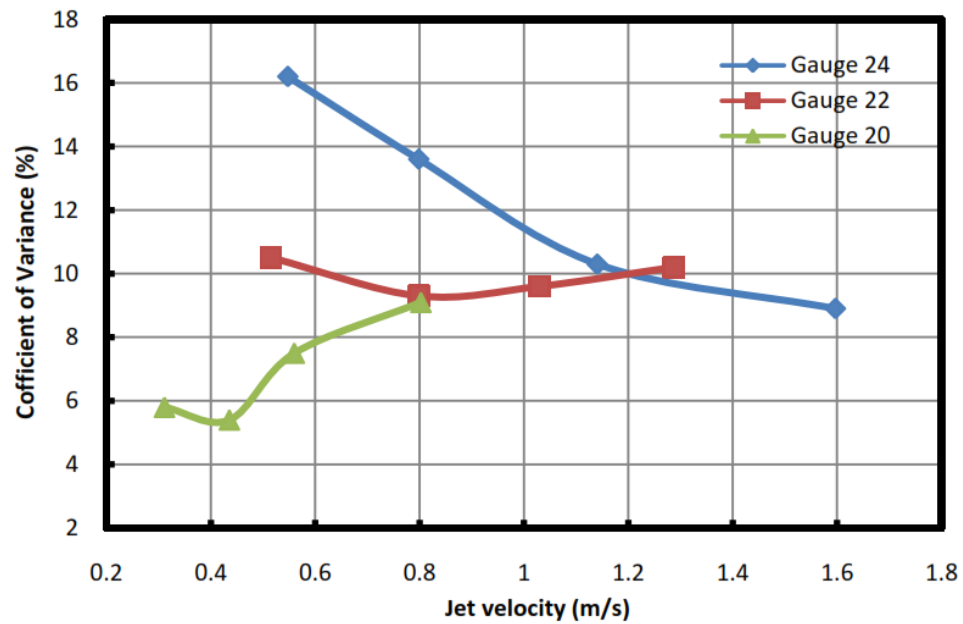


**Figure 2.6** Effect of jet velocity on particle size distribution

The effect of jet velocity on particle size distribution for different nozzle sizes is presented in Figure 2.6. The nozzle has 3 sizes which are 20 gauge, 22 gauge and 24 gauge ordered from large to small size. For the smallest nozzle (24 gauge needle), CV decrease in increasing jet velocity. In other hand, the largest nozzle (20 gauge needle), CV increase when the jet velocity increases.

### Influence of nozzle size

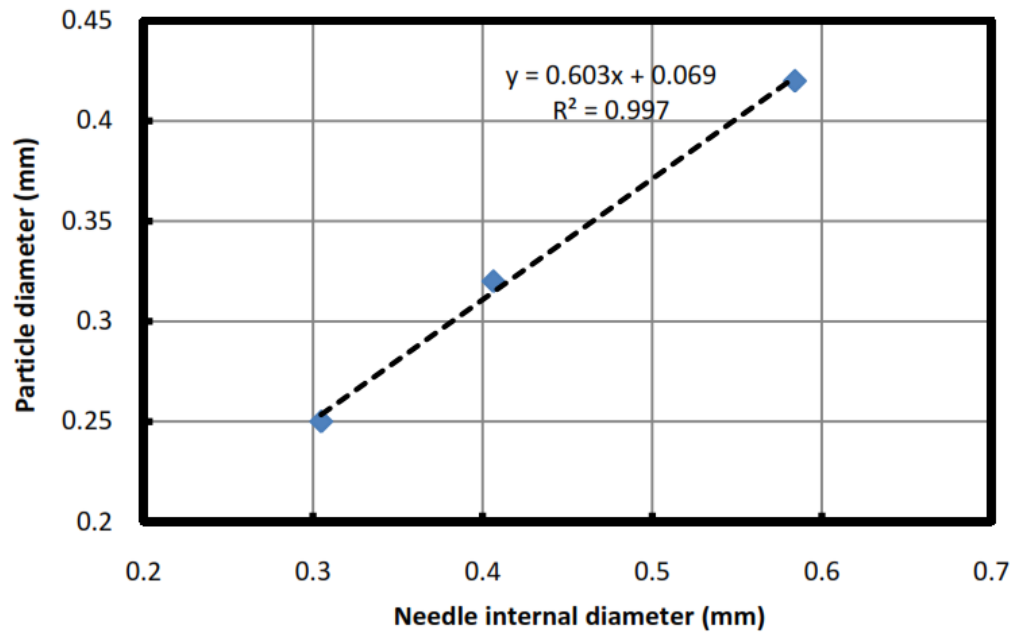


**Figure 2.7** Relationship between nozzle size and particle size

All previous researchers have established that the size of the nozzle from which the jet is formed is linearly related to the mean size of the droplets from laminar jet break-up, and that the nozzle size has by far the largest influence on the droplet size. Figure 2.7 confirms the linear relationship between the nozzle size and the particle size.

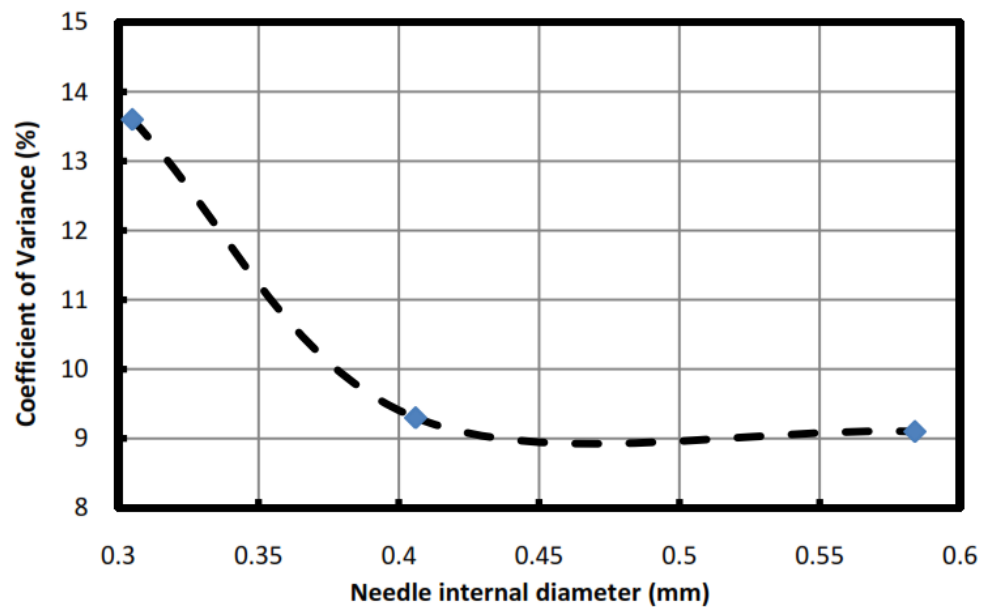


**Figure 2.8** Effect of nozzle diameter on particle size distribution



The effect of nozzle size on the particle size distribution is shown in Figure 2.8. It can be seen that, at a constant jet velocity (0.8 m/s) and jet phase viscosity (1.24 mPaS), the uniformity of the particles from the jet break-up improves with the coefficient of variance decreasing with increasing nozzle size. It should be noted, however, that the rate of improvement is significantly slower when the size of nozzle increased from 0.406 to 0.584 mm. If the size of the nozzle were to increase further, it is likely that the CV could start to increase again.

### **Influence of jet phase viscosity**

Viscous force of the jet phase plays an important role in the break-up process. In the previous two sections, the results were all from the break-up of DCM jets containing 3% w/v PCL, i.e. at a constant viscosity of the jet and the surrounding aqueous phase.

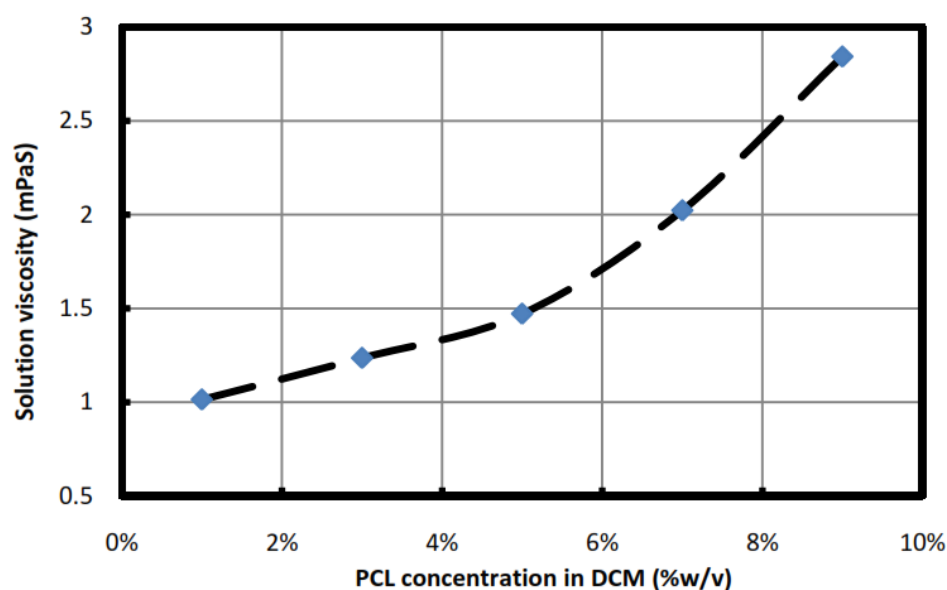


**Figure 2.9** Effect of PLC concentration on jet phase viscosity

In this section, the viscosity of the jet phase is changed by changing the PCL concentration in DCM. The relationship between the jet phase viscosity and the PCL concentration in DCM is shown in Figure 2.9.

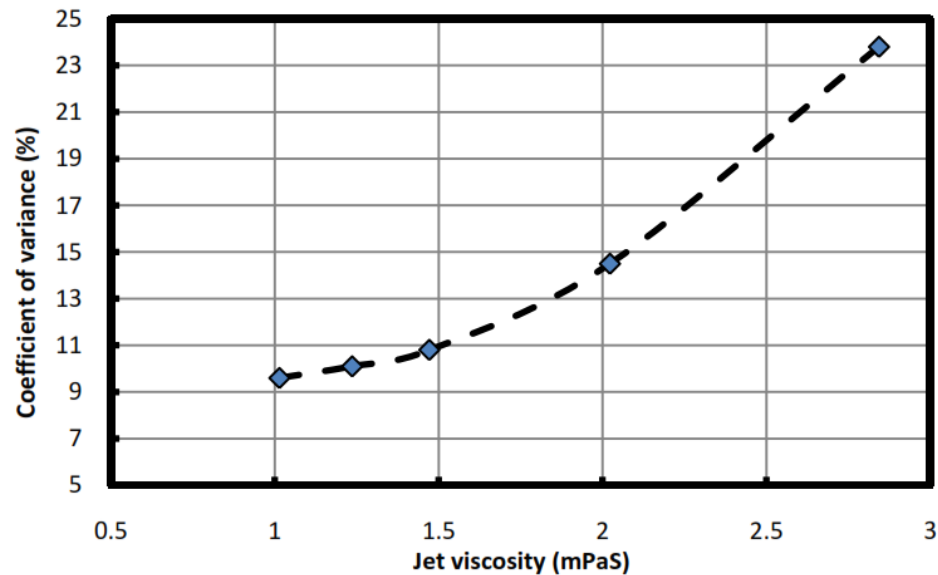


**Figure 2.10** Effect of jet phase viscosity on particle size distribution

Figure 2.10 shows the particle size uniformity results obtained from jetting the PCL solution through a 22 gauge needle at a linear velocity of 1.0 m/s. This result is consistent with both the theoretical and experimental findings by previous researchers that higher jet phase viscosity makes the jet break-up process more difficult. The difficulty is reflected in the broadening of the particle size distribution.

#### **2.4.2 Nucleation of Alpha lactose monohydrate induced using flow through a venturi orifice <sup>[7]</sup>**

Nucleation is a determinant of the final crystal size distribution produced during a crystallization process. Other studies in the literature have shown that mixing influences alpha lactose monohydrate nucleation. To investigate this in more detail, three different sized Venturi orifices were used to provide a point of passive mixing for supersaturated lactose solutions. This system allowed the study of different factors associated with characterizing the mixing process, including cavitation, power input, Reynolds number and vortex formation. A strong relationship was found between the number of vortices created in the system and the nucleation rate. It is speculated that the vortices decrease the distance required for diffusion of molecules in the system, increasing the rate at which they can come together to form a stable nuclei.

### Influence of Reynolds number

Using the idea that that flow instability is important in determining how mixing changes the nucleation rate, the relationship between the Reynolds number and the number of crystals formed was examined in Figure 2.12. The Reynolds number was calculated at the orifice of the Venturi.

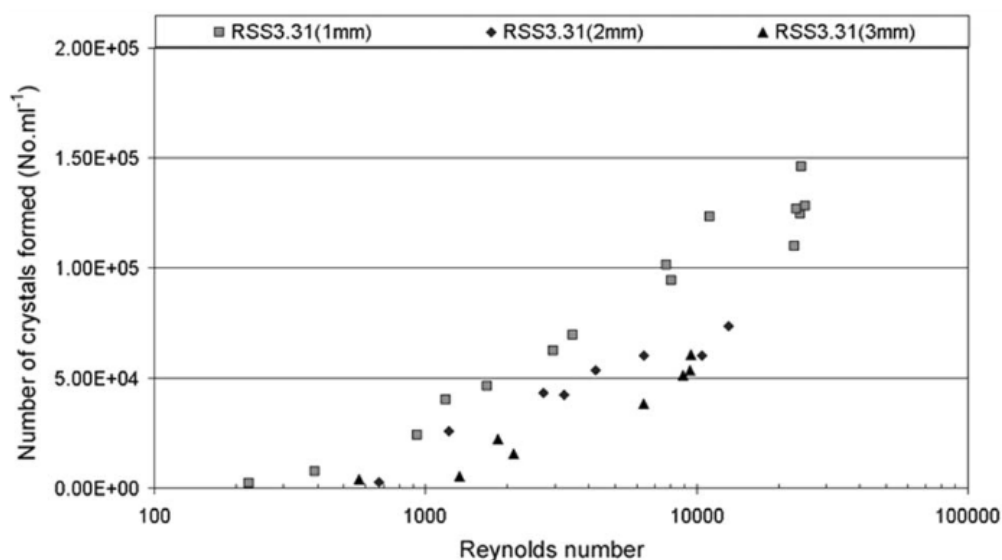


**Figure 2.11** Comparison of the Venturi orifice diameter on the number of crystals per ml at different Reynolds numbers (log scale).

Figure 2.11 show a similar pattern seen when examining the power input as a variable. As the only variable that has been changed in both situations is the fluid velocity. Once again, the smaller orifice diameter shows increased nucleation when a single Reynolds number is considered. The orifice diameter changes the Reynolds number where flow instability occurs. A narrowing of the flow constriction decreases the Reynolds number required for flow instability, and increasing the length of the constriction increased the Reynolds number required for flow instability. If flow instability is required for mixing to begin to influence the nucleation process, the intercept of the plots with the x-axis should provide an indication of the flow rate where the flow exiting the Venturi ceases to be laminar. The flow instability should begin at progressively decreasing Reynolds numbers as the diameter of the orifice is reduced.

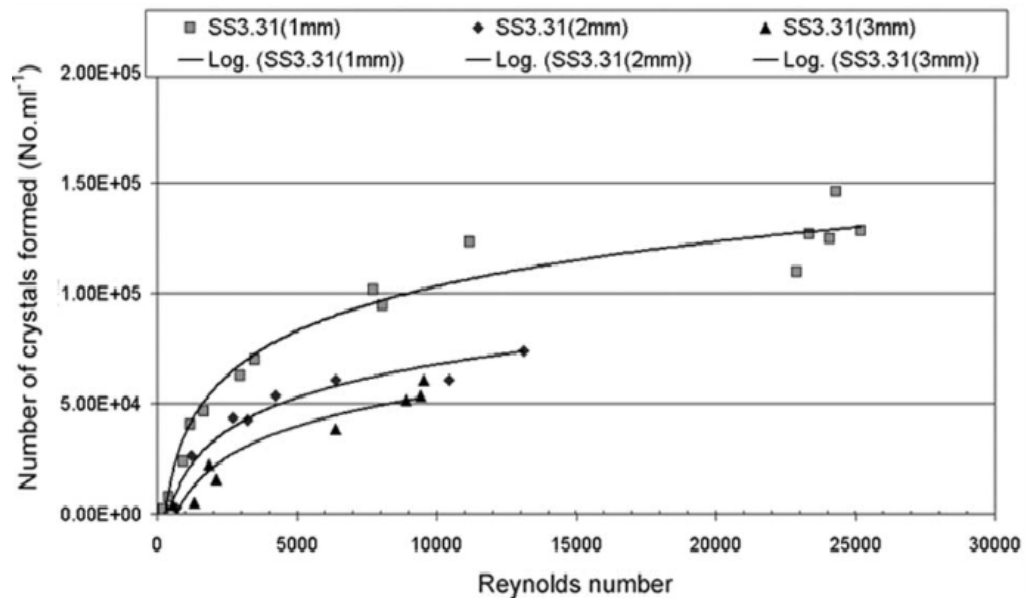


**Figure 2.12** Comparison of the Venturi orifice diameter on the number of crystals per ml at different Reynolds numbers (linear scale).

A log scale was used in Figure 2.11, making it easy to plot straight line through each data set. However, when viewed on a linear scale the extent of nucleation flattens out at higher Reynolds number with only small gains to be made by additional input as shown in Figure 2.12.

It can be observed that once the Reynolds number reached a critical value, the turbulence intensity became independent of the Reynolds number. Once the Reynolds number reached 5000, turbulence intensity reached a maximum. This provides an explanation for the results in 2.12.

### 2.4.3 Fully-Developed Flow in a Pipe: A CFD Solution <sup>[8]</sup>

A CFD model of the fully-developed laminar flow in a pipe is derived and implemented. This well-known problem is used to introduce the basic concepts of CFD including: the finite-volume mesh, the discrete nature of the numerical solution, and the dependence of the result on the mesh refinement. A MATLAB implementation of the numerical model is provided. Numerical results are presented for a sequence of finer meshes, and the dependency of the truncation error on mesh size is verified.

#### One-Dimensional Fully-Developed Flow

The left side of Figure 2.13 shows the geometry of a simple round pipe of radius  $R$ . The governing equation for fully-developed flow in a pipe is

$$\frac{\mu}{r} \frac{d}{dr} \left( r \frac{du}{dr} \right) - \frac{dp}{dx} = 0 \quad (1)$$

Where  $u$  is the velocity component along the pipe axis ( $x$  direction),  $\mu$  is the dynamic viscosity, and  $p$  is the pressure. The pressure gradient is a specified constant. The velocity is a function of  $r$  alone. The boundary conditions are

$$\left. \frac{du}{dr} \right|_{r=0} = 0 \quad (\text{Symmetry}) \quad (2)$$

$$u(R) = 0 \quad (\text{No slip}) \quad (3)$$

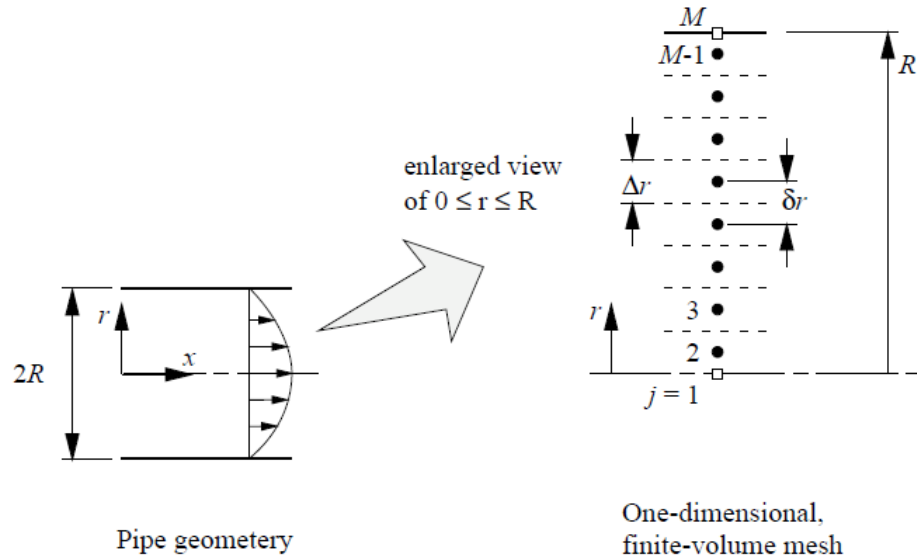


**Figure 2.13** Geometry of fully-developed flow in a pipe.

### Analytical Solution

The exact solution to Equation (1) subject to the boundary conditions is

$$u(r) = \frac{R^2}{4\mu} \left( -\frac{\partial p}{\partial x} \right) \left[ 1 - \left( \frac{r}{R} \right)^2 \right] \quad (4)$$

The maximum velocity in the pipe is at the centerline. Evaluating the preceding formula for  $r = 0$  gives

$$u_{\max} = \frac{R^2}{4\mu} \left( -\frac{\partial p}{\partial x} \right) \quad (5)$$

For a flow in the positive  $x$  direction,  $dp/dx < 0$ . Combining Equation (4) and (5) gives a more compact expression for the velocity profile.

$$u(r) = u_{\max} \left[ 1 - \left( \frac{r}{R} \right)^2 \right] \quad (6)$$

The average velocity in the pipe is

$$u_{ave} = \frac{1}{A} \int_A u dA = \frac{1}{\pi R^2} \int_0^R u 2\pi r dr \quad (7)$$

$$\begin{aligned} &= \frac{u_{\max}}{R^2} \int_0^R \left[ 1 - \left( \frac{r}{R} \right)^2 \right] r dr \\ &= \frac{u_{\max}}{2} \end{aligned} \quad (8)$$

The shear stress at the wall is

$$\tau_w = \mu \left| \left( \frac{du}{dr} \right)_{r=R} \right| \quad (9)$$

The absolute value sign is necessary because  $du/dr$  is negative at the wall. Using Equation (6) in Equation (9) gives

$$\tau_w = \mu \left| - \left( \frac{2u_{\max}}{R} \right)_{r=R} \right| = \frac{4\mu u_{ave}}{R} \quad (10)$$

The definition of the Darcy Friction factor is

$$f = \frac{8\tau_w}{\rho u_{ave}^2} \quad (11)$$

Substituting Equation (10) into Equation (11) gives

$$f_{pipe} = \frac{32\mu}{\rho u_{ave} R} = \frac{64}{\text{Re}}$$

or

$$f_{pipe} \text{Re} = 64 \quad (12)$$

$$\text{Re} = \frac{\rho u_{ave} D}{\mu} \quad (13)$$

is the Reynolds number.

This literature also used the CFD technique to solve the problem of the fully-developed flow in pipe. These equations are derived for predicting the fluid flow. The velocity and the Reynolds number can be calculated by equation (6) and (13). However, they are quiet simplified equation and geometry than this thesis, but similar in the principle.

## **CHAPTER 3 METHODOLOGY**

The thesis is required the systematic methodology to effectively achieve the work on time. This chapter describes steps for doing a thesis, the details of each step including how to perform experiments to verify the accuracy of a CFD model.

### **3.1 ANSYS FLUENT software**

The first step is studying the fundamental knowledge that is useful to do a thesis. There are two topics to be understood before beginning as the following, literature review, which is searching previous literatures associated with CFD models for the laminar flow situation. Another topic is learning how to use a CFD simulation tool or the Fluent 6.0. It can be found in the Fluent software: Help toolbar > PDF > Tutorial Guide.

Tutorial guide consists of 38 examples of the computational fluid dynamics problem, which varies according to the purpose, and nature of flow situations. The setting in FLUENT software is different too. There are two examples that are similar to the characteristic of background of this thesis such as Chapter 1: Introduction to Using ANSYS FLUENT in ANSYS Workbench: Fluid Flow and Heat Transfer in a Mixing Elbow and Chapter 3: Introduction to Using ANSYS FLUENT: Fluid Flow and Heat Transfer in a Mixing Elbow.

In addition, It should take action to study how to create a model for the dynamics of flow to become familiar with the use of this program even more.

### **3.2 Input data preparation**

After using a CFD simulation tool is known, the required data, which have to be entered into the software, is also recognized. At this step, it is the collection of data used to create CFD models. For examples, the geometry of a vertical column, the dimension of three inlet types such as 16-pipes inlet, one pipe upward inlet and one pipe sideward inlet and the physical properties of fluid etc. For more details of these, (See Appendix A).

Moreover, there are also governing equation and boundary condition, which are important to generate the model. These data can be gathered from a real operation, relevant literatures and experts.

### **3.3 Creation of CFD models**

In this step, ANSYS Workbench V.13 is used to create the CFD model for the fully-developed laminar flow. Instead of using Fluent 6.0 directly because, it is easier to manage files. There are three inlet designs in order to test the capability of the fully-developed



laminar flow in a vertical column. Thus, all of inlet designs are created for comparison. However, the process of modeling is the same and there are five steps as shown in following figure.

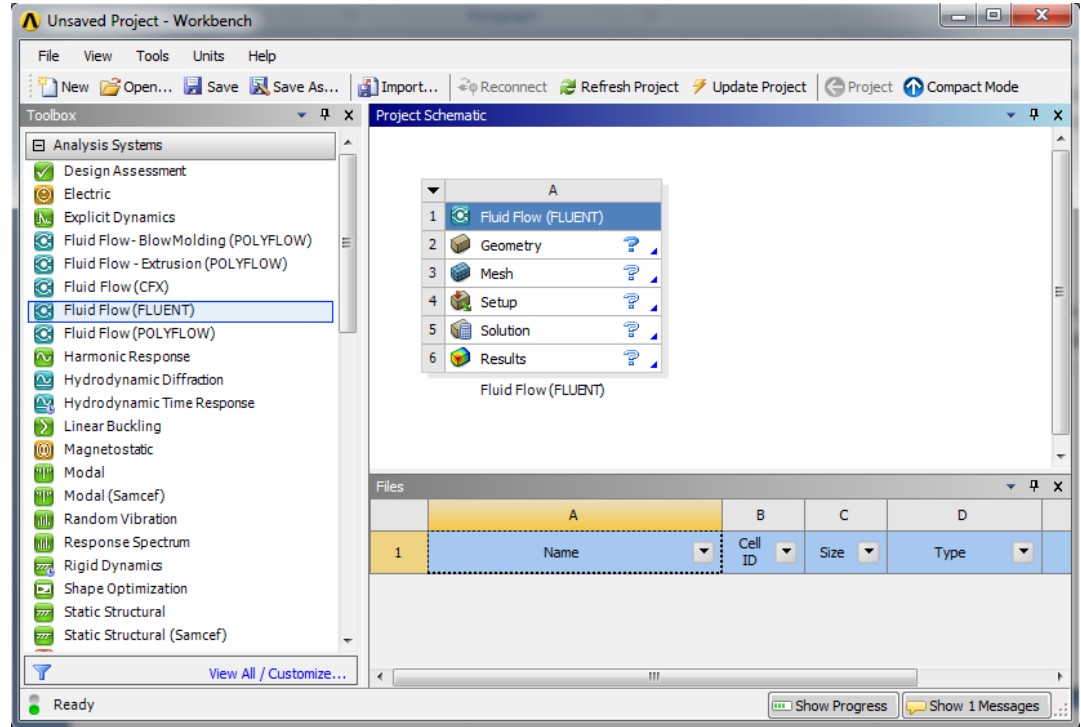


**Figure 3.1** The project schematic of ANSYS Workbench

The first step is to draw the **geometry** of the system in Design Modeler program. The second step is “**Mesh**” which divides the system into several small volume elements. For next step is “**Setup**”. In this process, governing equations, properties of material and boundary conditions will be defined completely in order to get the simulation results accurately as much as possible. After that, the model is calculated in a **solution** step and Fluent 6.0 is utilized for two of these steps. The last step is “**Results**” which is analyzing simulation results by using CFD-post process and described in the next paragraph.

### 3.4 Analysis and interpretation of CFD simulation results

The simulation results will be analyzed with the CFD-post process software. From the purpose of this thesis, velocity profiles of fluid inside a vertical column at different height around the feed inlet have to be presented in order to compare together. The most appropriate inlet is the inlet, which is able to develop the laminar flow profile at the lowest position. In addition to observing the velocity profile, streamline of fluid is also useful to design the inlet to distribute the flow of fluid that enters into the column.

### 3.5 Validation of the simulation results with experimental data

Experiments are conducted in a laboratory using a vertical column and various inlets same as the actual work. Experimental results are recorded and used to check the accuracy of the simulation results. The experiments for the fully-developed laminar flow in a vertical column with different feed inlet designs are described in the next section

The following diagram is the methodology of thesis.

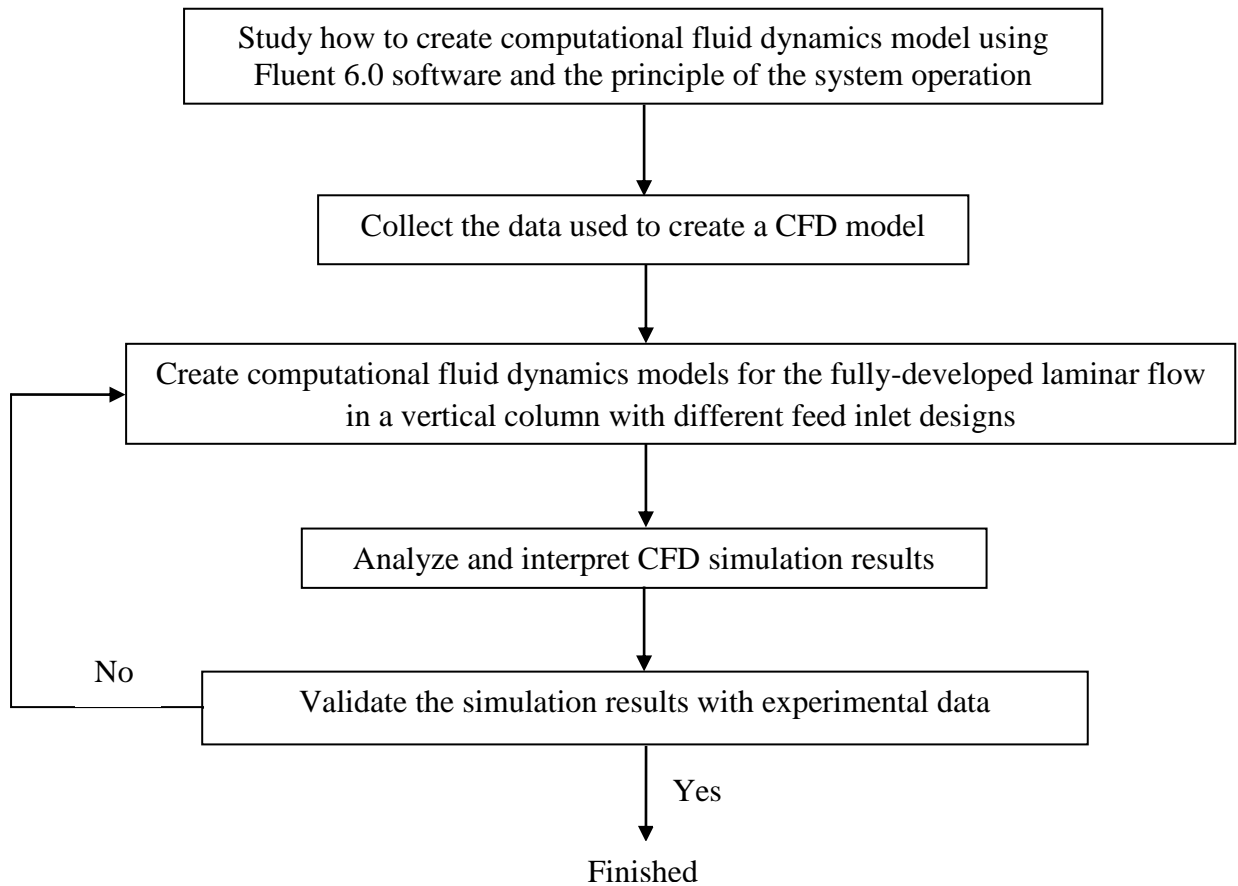


**Figure 3.2** Methodology

## **CHAPTER 4 RESULTS AND DISCUSSION**

In the previous chapter, the steps to create CFD models for the fully-developed laminar flow of each feed inlet are described. In this chapter, the simulation results and the analysis are discussed. Firstly, the study of the effect of the number of meshes on the accuracy of simulation results was done by changing the order of spatial discretization and increasing the number of meshes. Secondly, the geometry of the system was adjusted in order to make the CFD models more realistic by adding a cone shape at the bottom of the column.

After that, velocity profiles at various heights are plotted in order to reveal the height at fully-developed laminar flow profile of each inlet. This height or y-distance is measured from the reference level (See Appendix A)

The most important step is to validate CFD models with experimental data. Experiments provided the information of the fluid flow inside the vertical column with three different inlet designs. During experiments, dye was used to observe the fluid flow behavior at the steady-state condition. The flow patterns of dye are recorded by video cameras and experimental data are shown in Appendix C.

The results and discussion are presented as the following topics.

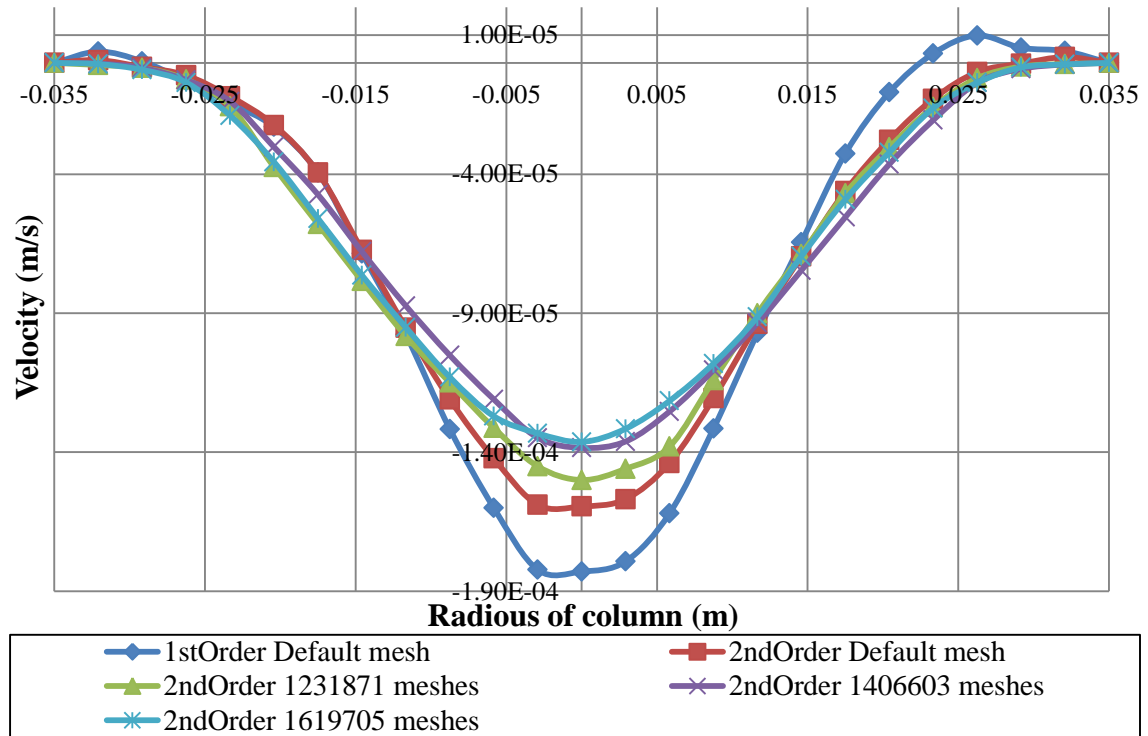
- a) The effect of the number of meshes on the simulation results.
- b) The velocity profiles of fluid near a fully-developed laminar flow.
- c) The results of various inlets are compared to find out which one can develop the laminar flow at the lowest position.
- d) Validation of CFD models with experimental data.

There are three inlet designs listed below. (See more details in Appendix A)

- 1) 16-pipes inlet
- 2) One pipe upward inlet
- 3) One pipe sideward inlet
- 4) New one pipe inlet

## 4.1 16-pipes inlet

### 4.1.1 The effect of the number of meshes on the simulation results



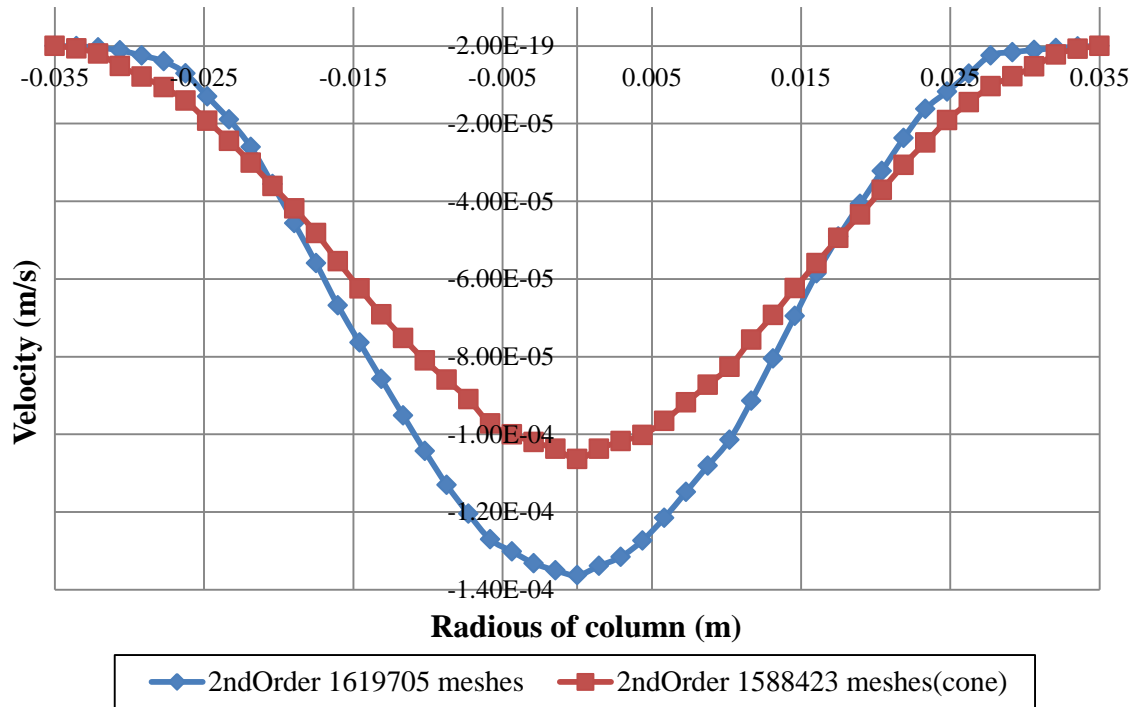
**Figure 4.1** The velocity profiles of fluid at the bottom of the column using different in spatial discretization and the number of meshes

Figure 4.1 shows a velocity of fluid at the bottom of the column using 16-pipes inlet throughout a radius. Each line in the figure represents simulation results using different the order of spatial discretization and the number of meshes. Initially, a CFD model has the number of meshes about 680,000 meshes as a default of program and uses the first-order spatial discretization to calculate a solution which is a dark blue line. After that, the model is changed a discretization scheme from first-order to second-order and then calculated again. The results are shown as the red line. It seems that the simulation results of both cases are significantly different. Since the first-order scheme generally converges the criteria faster than the second-order scheme but it also gives less accurate results. Therefore, the simulation result from second-order (a red line) discretization is more accurate than other one (a dark blue line).

Thereafter, the effect of the number of meshes on the simulation results was studied. The number of meshes of CFD model is increased as shown in green, purple and blue lines, which equal to 1.2, 1.4 and 1.6 million meshes; respectively, because increasing the number of meshes makes the calculation more accurate. It can be observed the deviation between

the green line and the purple line because the number of meshes still effects in this range. However, a gap among a purple line and a blue line is minimal. It is also called the mesh independent solution. Therefore, the model representing in a blue line can give the best solution. This mesh number will be used in the following study.

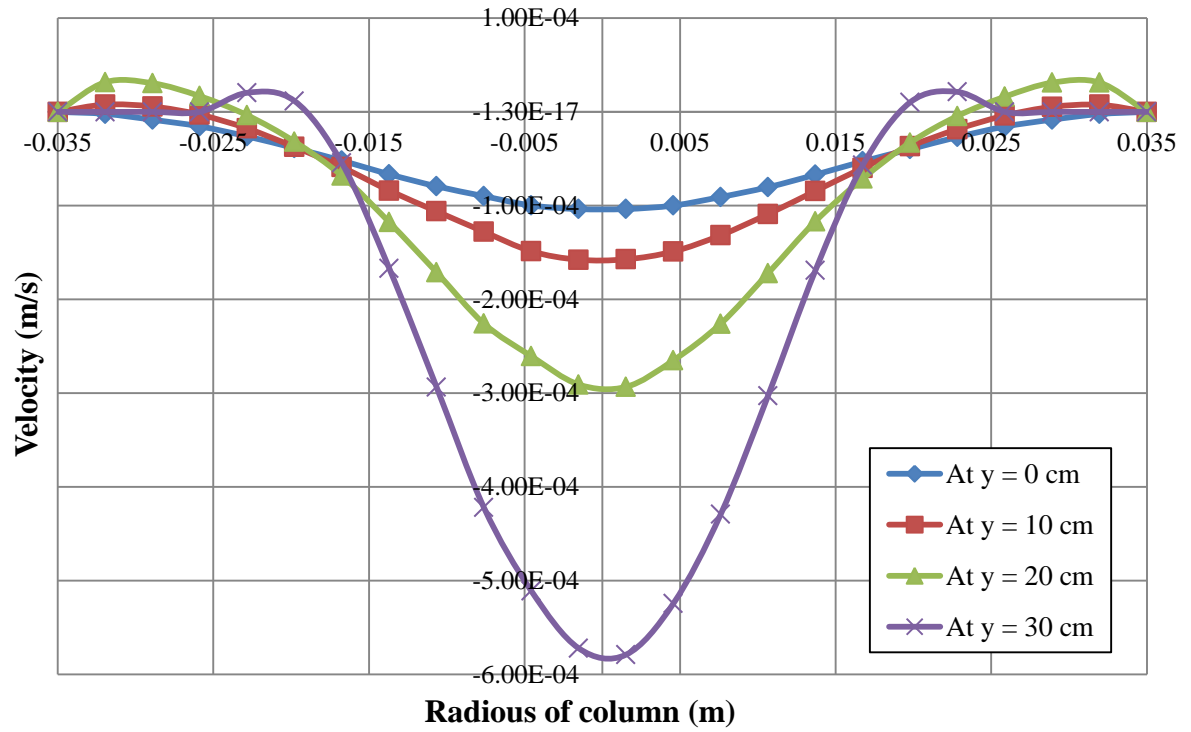
#### 4.1.2 Development of the geometry of a vertical column



**Figure 4.2** The velocity profiles of fluid at the bottom of the column with and without a cone shape

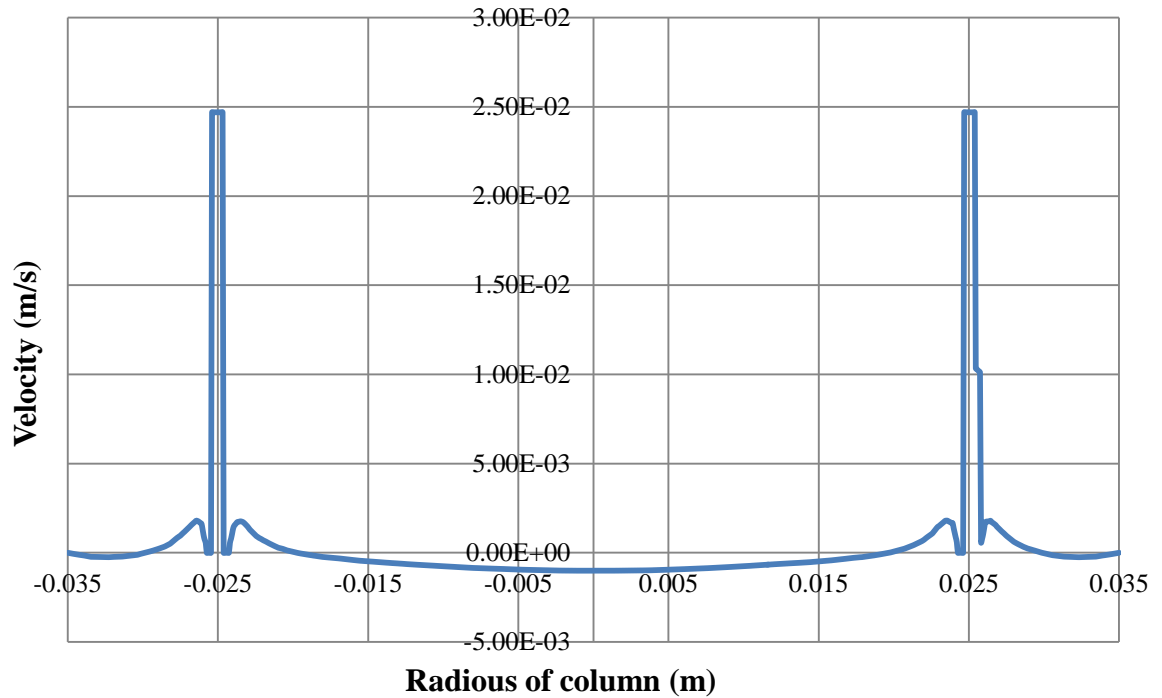
In order to make the model more realistic, a researcher has to prepare the actual tool in the laboratory. It found that a geometry at the bottom of a vertical column having a cone shape. Thus, the geometry in a CFD model has to be adjusted by adding the part of cone. The simulation results are shown in Figure 4.2. The CFD model using second-order discretization and 1.6 million meshes with and without the cone shape represents as the blue line and the red line. It can be observed that those lines clearly distinguish. Owing to the position of a cone shape, which is at the bottom of the column and near the feed inlet, it cannot be neglected because it gives the direct effect to the outlet boundary condition of the system.

### 4.1.3 The velocity profiles of a fluid at various heights of a vertical column



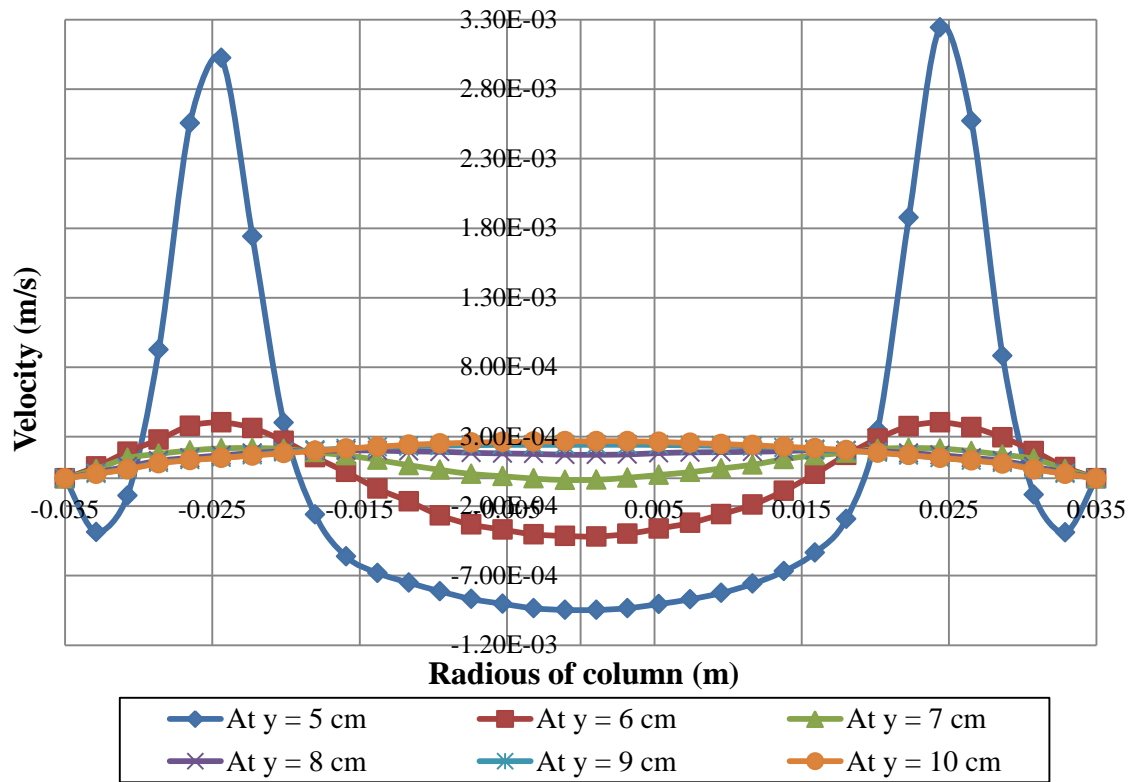
**Figure 4.3** The velocity profiles of fluid at the position below a feed inlet

Figure 4.3 shows the fluid velocity at the different height below the feed inlet. The y-distance shows a height in the vertical, which is measured from the reference as Appendix A. In this figure, the purple line shows the velocity profile at the nearest position to the feed inlet has the highest velocity. Noticed that the effect of the height on the fluid velocity. The fluid flows pass though the column, the velocity decreases due to the effect of no slip wall.



**Figure 4.4** The velocity profiles of fluid at the position of a feed inlet

Figure 4.4 shows the fluid velocity profile at the position of 16 pipes feed inlet. The distance of inlet position from the reference level is around 4 cm as shown in Appendix A. The velocity profiles have two peaks because the system has two pipes inlets in the same plane. The peak locates at radius equal to -2.5 cm and 2.5 cm due to the inlet pipe extends from the wall 1 cm ( the wall locate at  $r = -3.5$  cm and  $r = 3.5$  cm).



**Figure 4.5** The velocity profiles of fluid at the position above a feed inlet

The highlight of this research is the height to develop the fully laminar flow. Nevertheless, it is not clear to identify the position that the fluid reaches the stable laminar profile. Therefore, the velocity profiles of the fluid at the positions around the top of a feed inlet are shown in Figure 4.5. The blue line has the highest velocity due to its position is the closest to the inlet. Moreover, the fluid velocity will decrease along the fluid flows up the column because of the wall effect (no slip wall). However, the fluid flow is quite the same velocity at 9 and 10 cm heights (measured from the reference level) because the fluid starts to develop to the stable laminar profile. Thus, the velocity profile at 9 and 10 cm. height ought to be studied further.



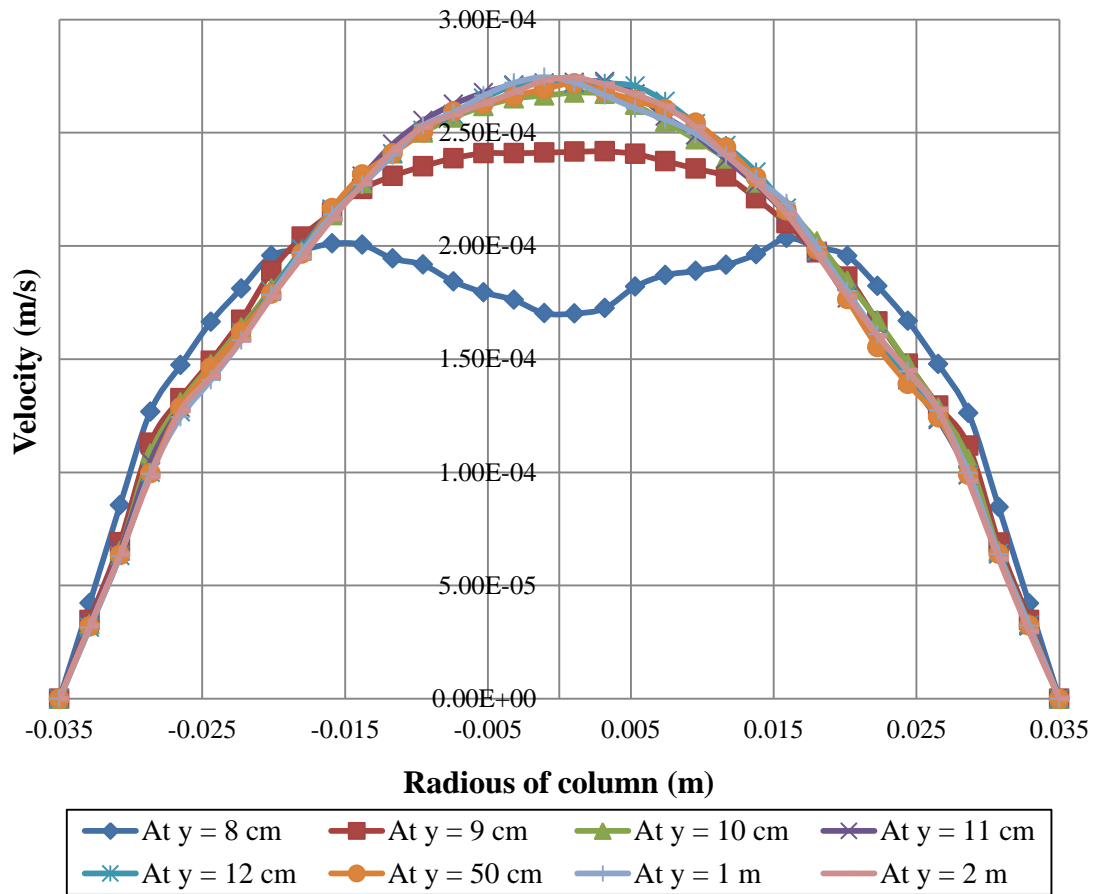


**Figure 4.6** The velocity profiles of fluid at the position near a fully-developed laminar flow

This figure shows the velocity profile of fluid at the different positions near the zone that the fluid fully developed to the laminar flow. One can notice that the green line locates at 10 cm. from the reference position. This is the last position before the fluid reaches the stability and the next line represents a laminar profile. Thus, it can be concluded that the fluid in the vertical column with the 16-pipes inlet is a fully developed to laminar flow at 11 cm. height.

## 4.2 One pipe upward inlet

### 4.2.1 The effect of the number of meshes on the simulation results

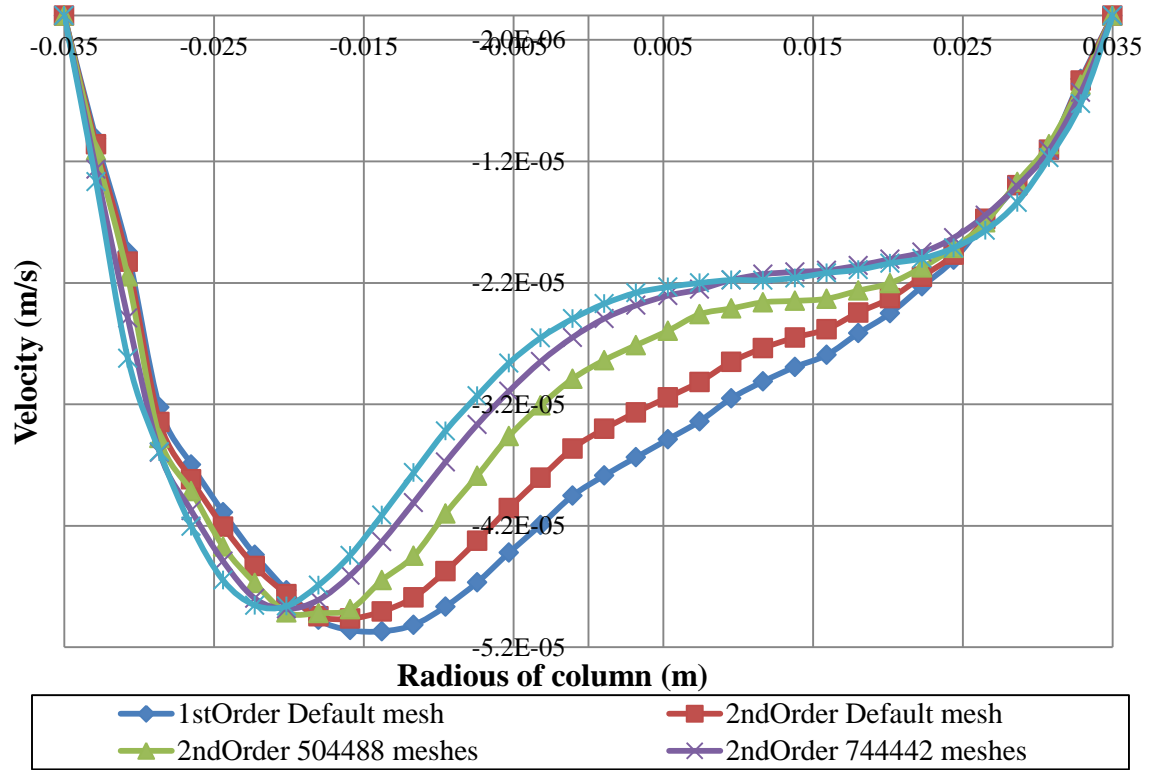


**Figure 4.7** The velocity profiles of fluid at the bottom of the column using different inspatial discretization and the number of meshes

In order to improve the accuracy of model for a laminar flow in a vertical column with the one pipe upward inlet, the spatial discretization is changed from first-order scheme to second-order scheme. Since the first-order scheme generally converges the criteria faster than the second-order scheme but gives less accurate results. Moreover, the mesh number is adapted also because the smaller volume elements can represent results that are more delicate. Therefore, the model has the various mesh number from 265,908 to 1,043,429 meshes. The calculation is more accuracy because of increment of the spatial discretization and number of mesh. The most accuracy shown in the lighter blue line represents the model of the second-order scheme and number of mesh around 1 million meshes. Thus, this model is used to analyze next.

#### 4.2.2 The velocity profiles of a fluid near a fully-developed laminar flow

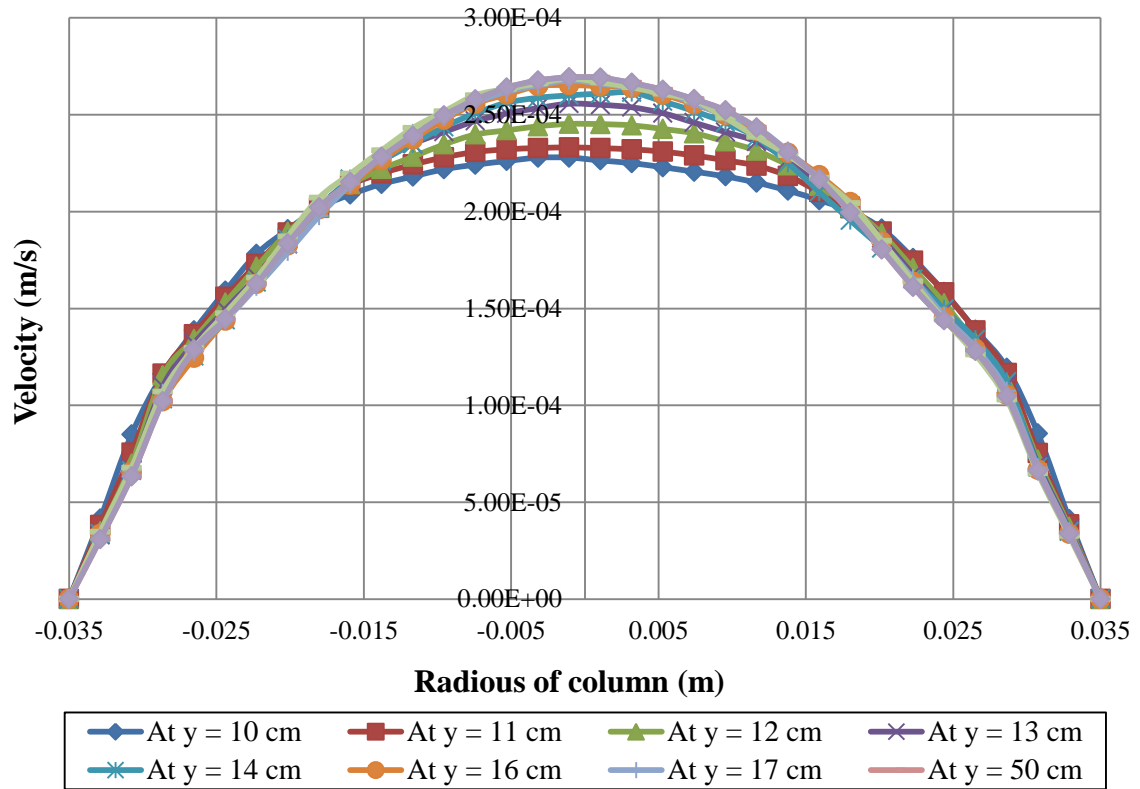


**Figure 4.8** The velocity profiles of fluid at the position near a fully-developed laminar flow

Figure 4.8 shows the velocity profile of fluid at the position near the zone is a fully-developed laminar flow in using one pipe upward inlet. Notice that the orange line locates at 16 cm. from the reference position is the last position before the fluid reaches the stability while the next line represents a laminar profile. Thus, it can be concluded that the fluid in the vertical column with the one pipe upward inlet is a fully developed laminar flow at 17-cm. height.

### 4.3 One pipe upward inlet

#### 4.3.1 The effect of the number of meshes on the simulation results

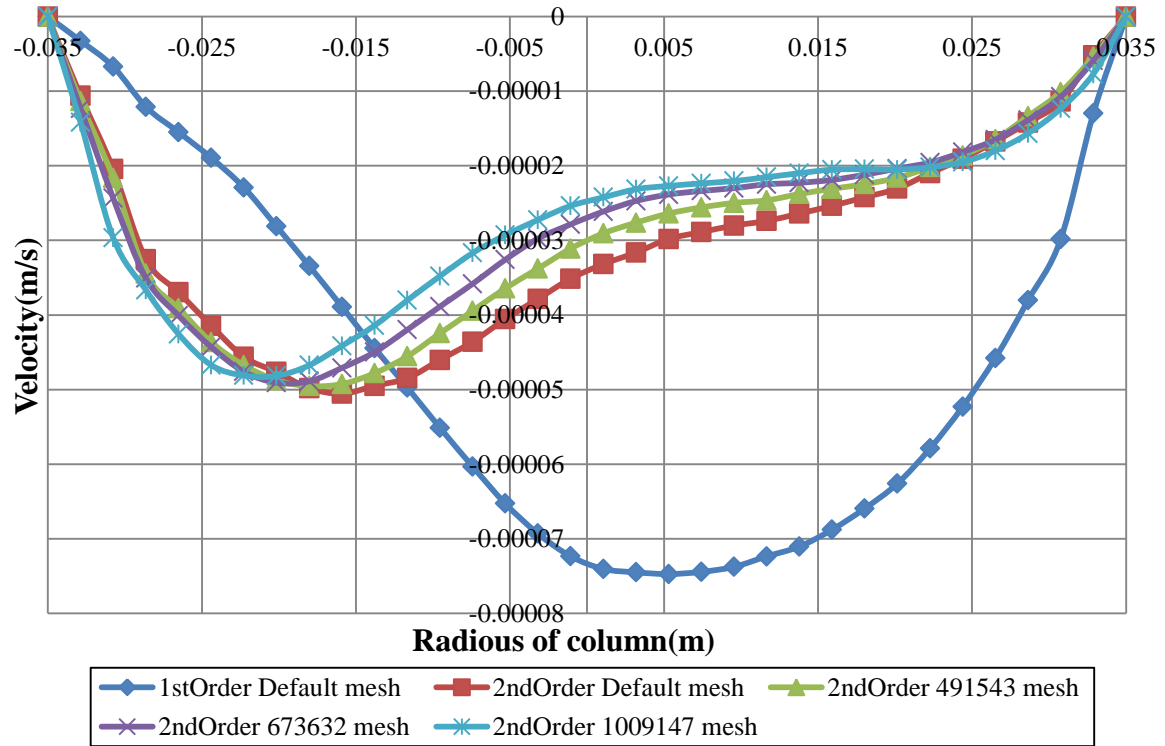


**Figure 4.9** The velocity profiles of fluid at the bottom of the column using different in spatial discretization and the number of meshes

In order to improve the accuracy of model for a laminar flow in a vertical column with the one pipe sideward inlet, the spatial discretization is changing from first-order scheme to second-order scheme. Since the first-order scheme generally converges the criteria faster than the second-order scheme but gives less accurate results. Moreover, the mesh number is adapted also because the smaller volume elements can give more delicate results. Therefore, the various mesh number from 491,543 to 1,009,147 meshes was performed. The calculation is more accuracy because of increment of the spatial discretization and number of mesh. The most accuracy shown in the lighter blue line, it represents the model of the second-order scheme and number of mesh around 1 million meshes. Thus, this model is used to analyze next.

### 4.3.2 The velocity profiles of a fluid near a fully-developed laminar flow

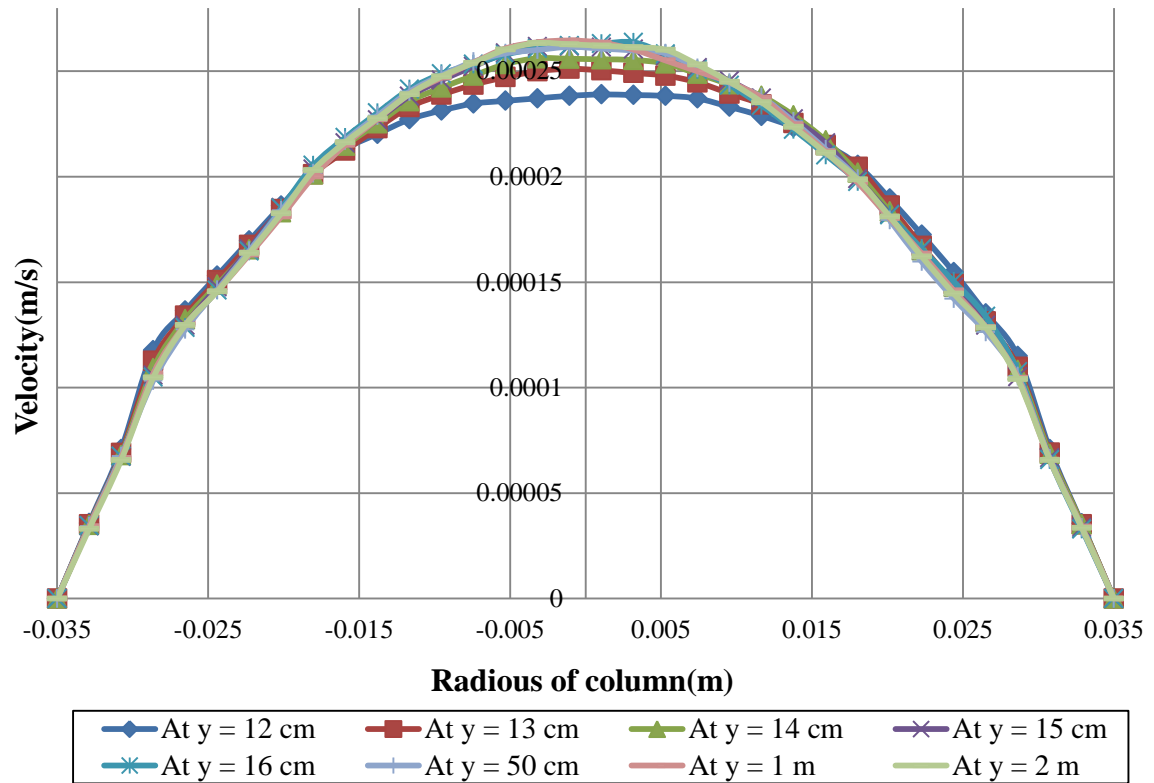
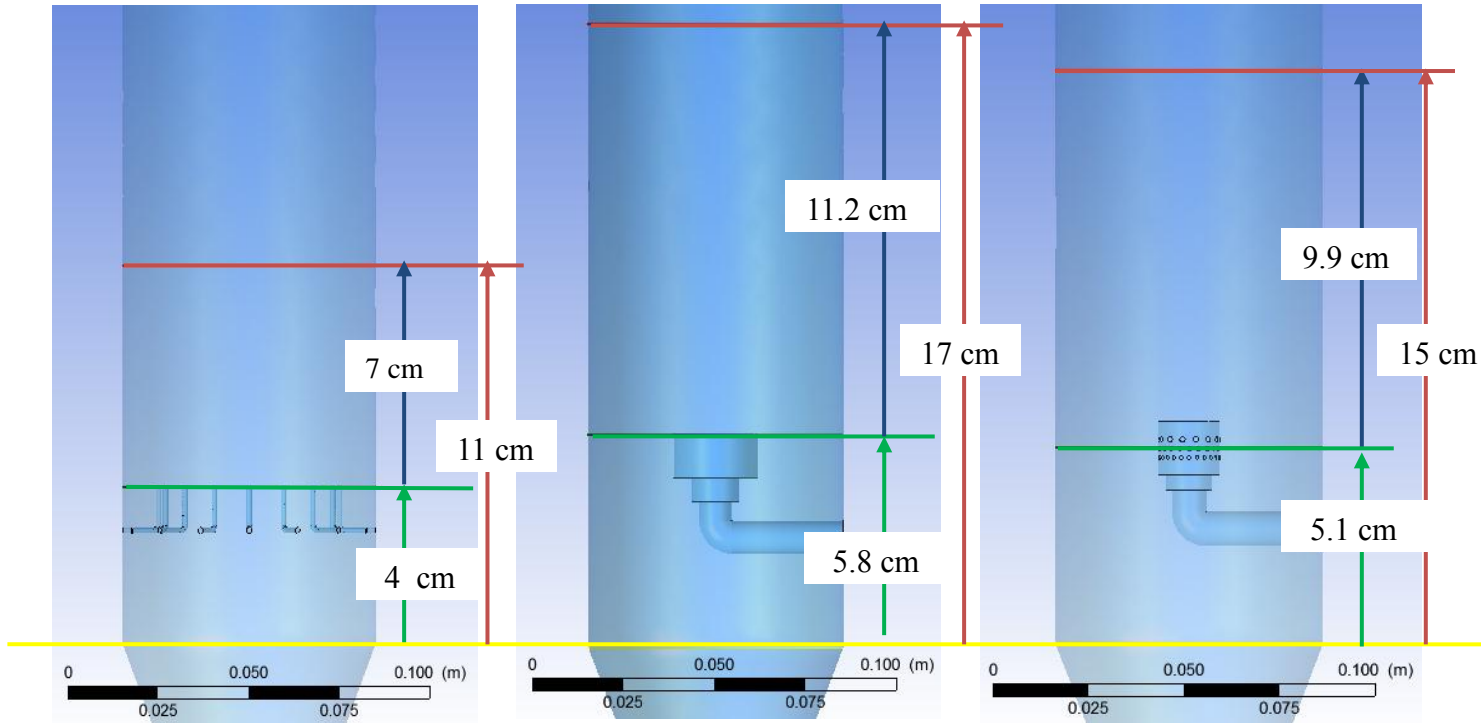


**Figure 4.10** The velocity profiles of fluid at the position near a fully-developed laminar flow

Figure 4.10 shows the velocity profile of fluid at the position near the zone is a fully-developed laminar flow in using one pipe sideward inlet. Notice that the dark green line locates at 14 cm. from the reference position is the last position before the fluid reaches the stability while the next line represents a laminar profile. Thus, it can be concluded that the fluid in the vertical column with the one pipe upward inlet is a fully developed laminar flow at 15-cm height.

## 4.4 All feed inlets

### 4.4.1 Comparison of the type of inlet developing the laminar flow at the lowest position



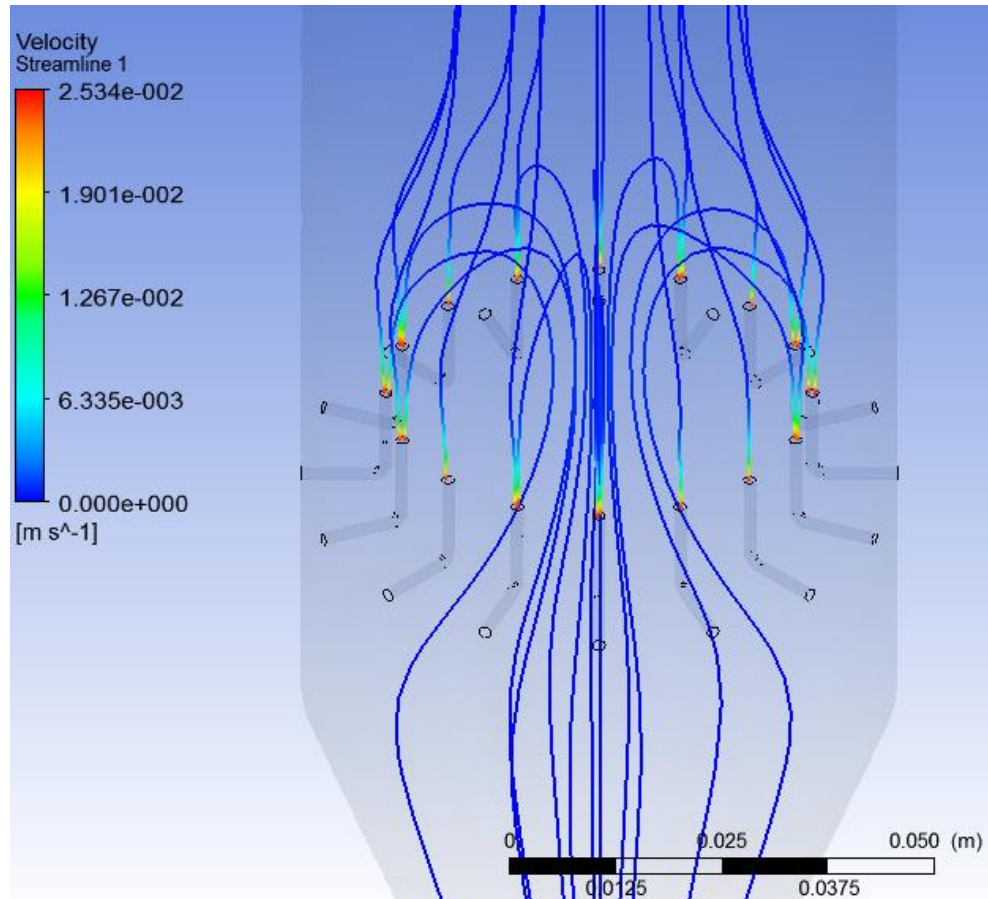
**Figure 4.11** The comparison of heights in which feed inlet designs develop the fully-developed laminar flow

Figure 4.11 shows the height of the feed inlets in the area of stable laminar profiles. The yellow line represents the reference level which  $y$  equals to zero. The red line shows the height of a fluid level that is the fully develop laminar flow comparing with the reference level, which is based on the analysis in the section c), e) and g) before. However, the height as shown in the red line cannot be used to compare directly because the position of each inlet is not the same as shown in the green line. The green line shows the height of the feed inlet compared with the reference level. Therefore, the height that fluid uses to develop to the stable laminar flow equal to the height at the laminar profile compared with the reference level (red line) subtracts the height of the feed inlet compared with the reference level (green line) as shown in the blue line.

It can conclude that the 16-pipes inlet provides the fastest fully-developed laminar flow fastest at 7 cm measured from the inlet. While the laminar profiles of one pipe sideward inlet and one pipe upward inlet are stable at 9.9 and 11.2 cm. from inlets; respectively.

#### 4.4.2 Validation of CFD models with experimental data

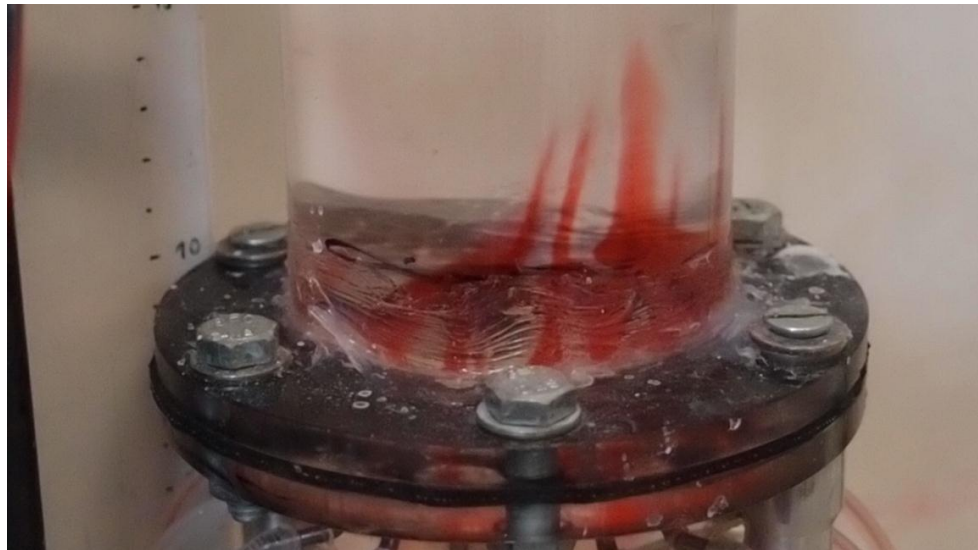
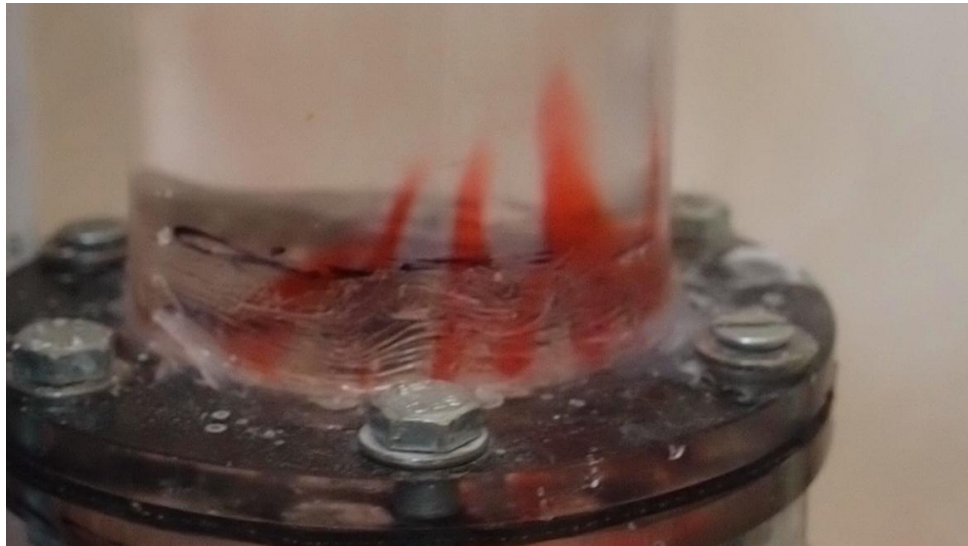
12(a)



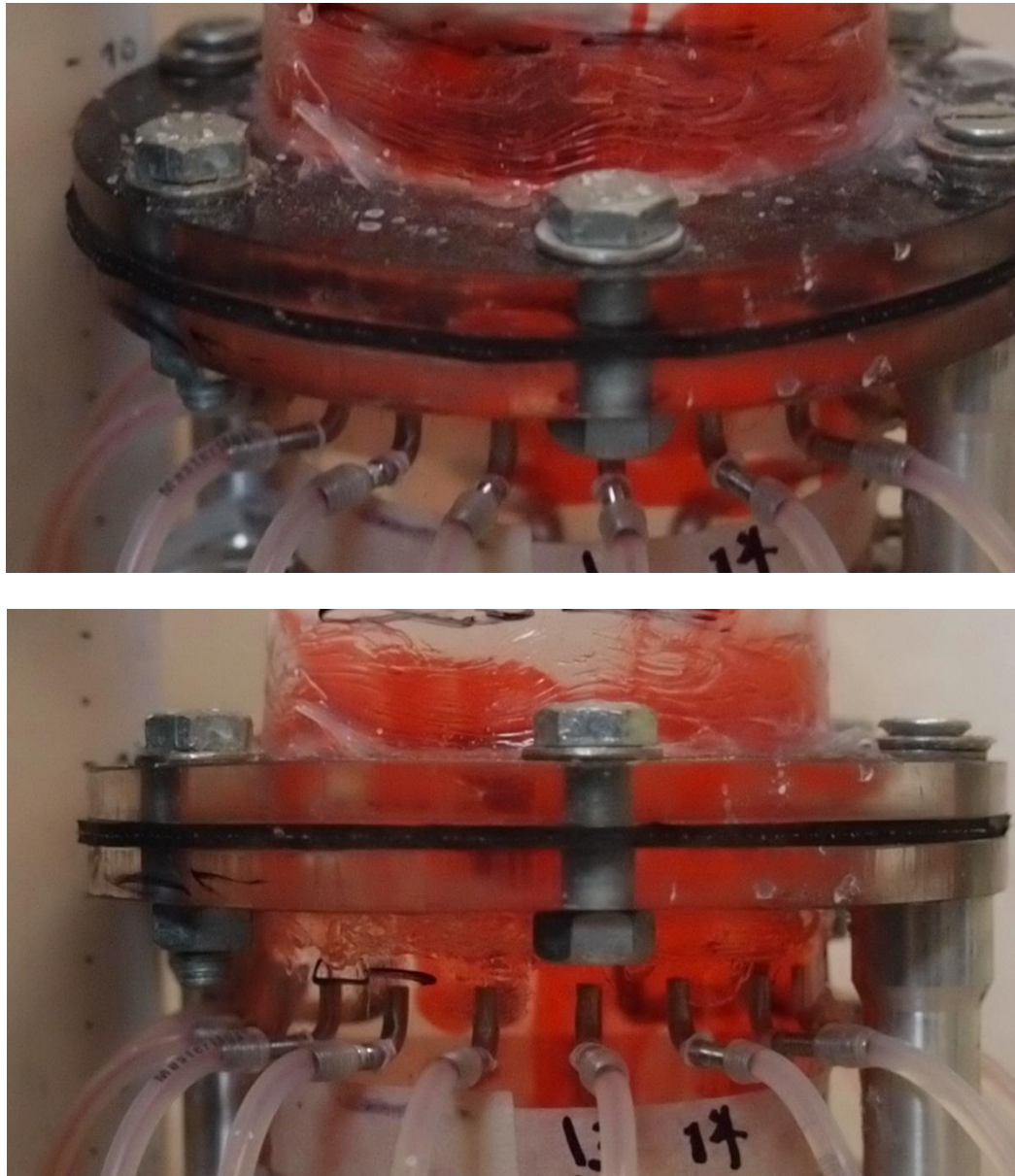
12(b)







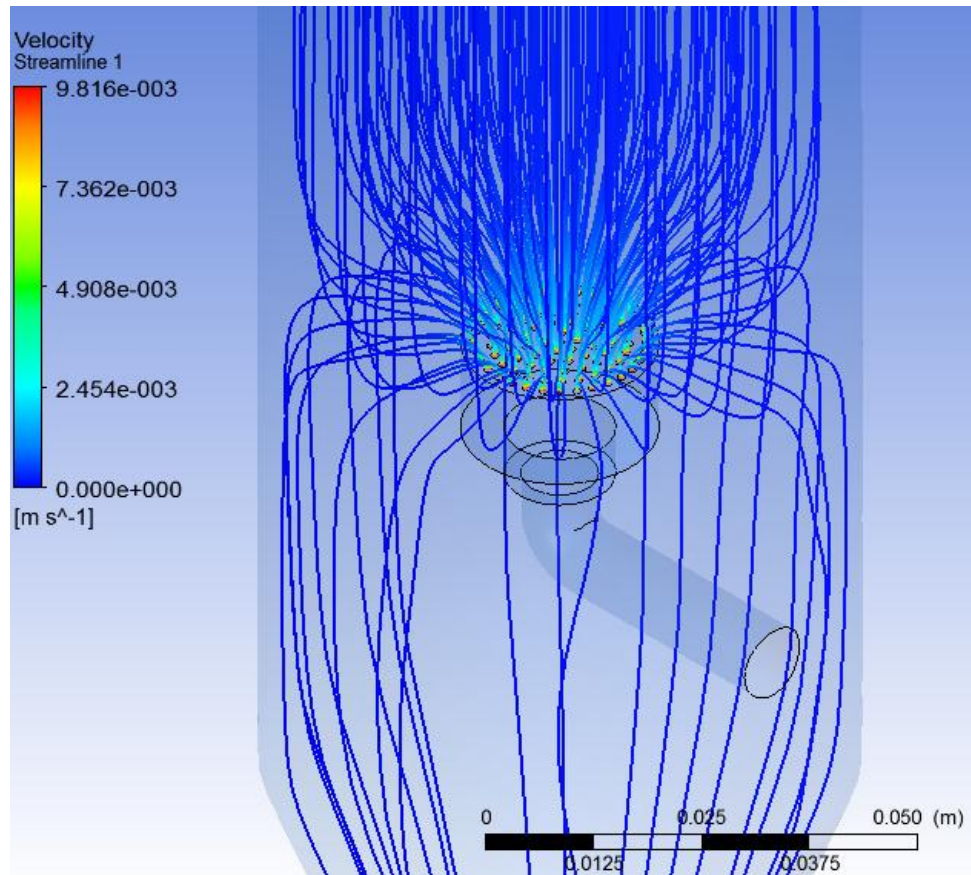




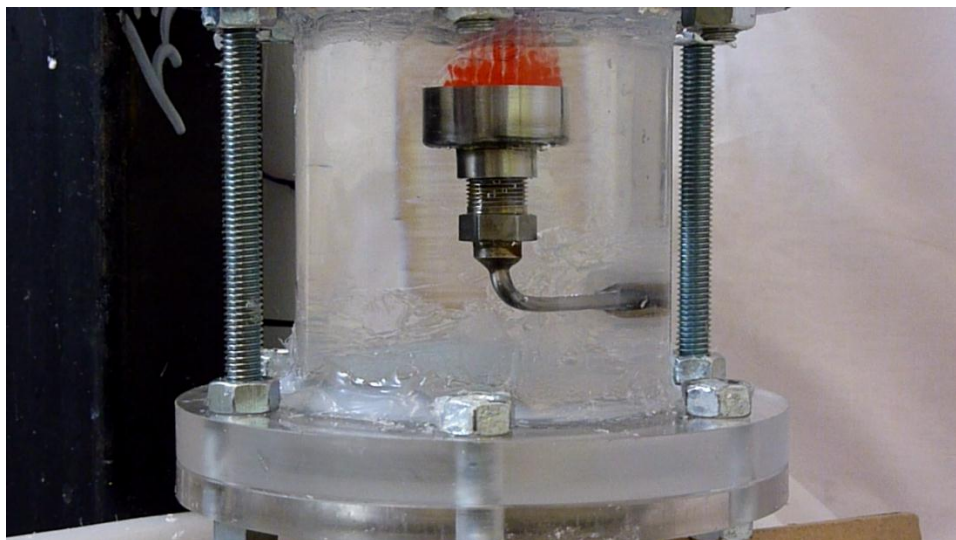
**Figure 4.12** The streamlines of fluid of a vertical column with 16-pipes inlet

Figure 4.12(a) shows the flow path of the fluid that was calculated from the simulation program and Figure 12(b) shows the flow path of dye, which was recorded from the experiment. The simulation found the most of fluid that was fed into the column will flow up to the top. Some of fluid will circulated to the center of the column and flows down to the bottom of the column, which is consistent with the experimental results. The experimental results show the flow path of fluid is similar to the simulation results but the flow path is not symmetry. Since the distributor that was used cannot distribute dye and the flow rate to all 16 inlet pipes ideally.

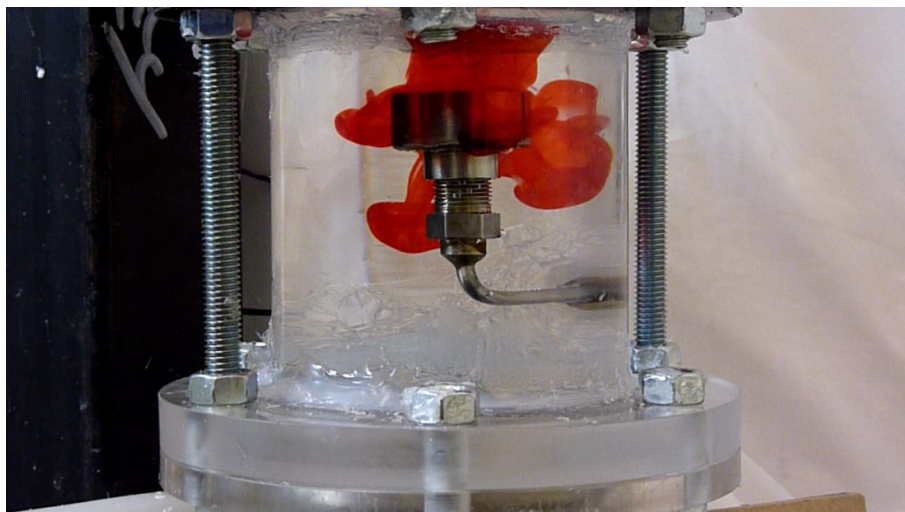
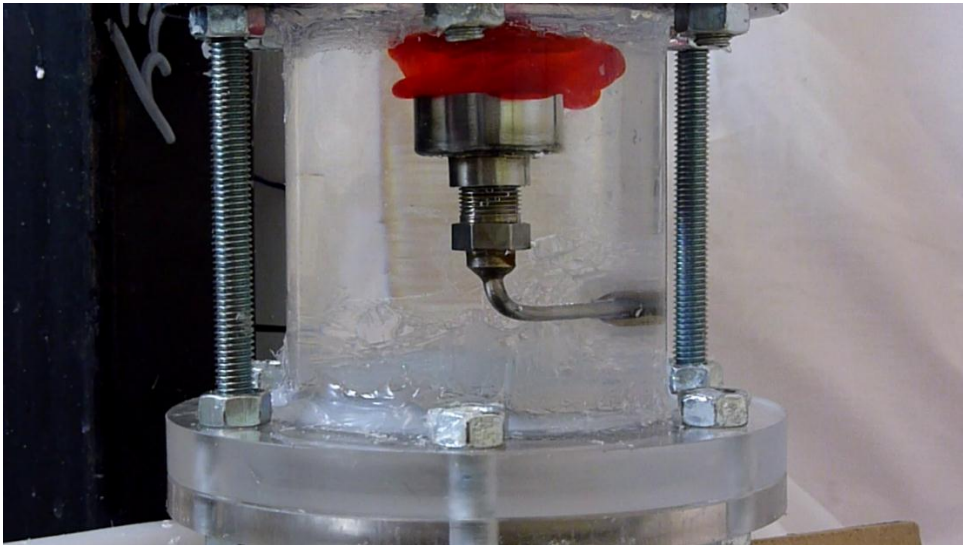
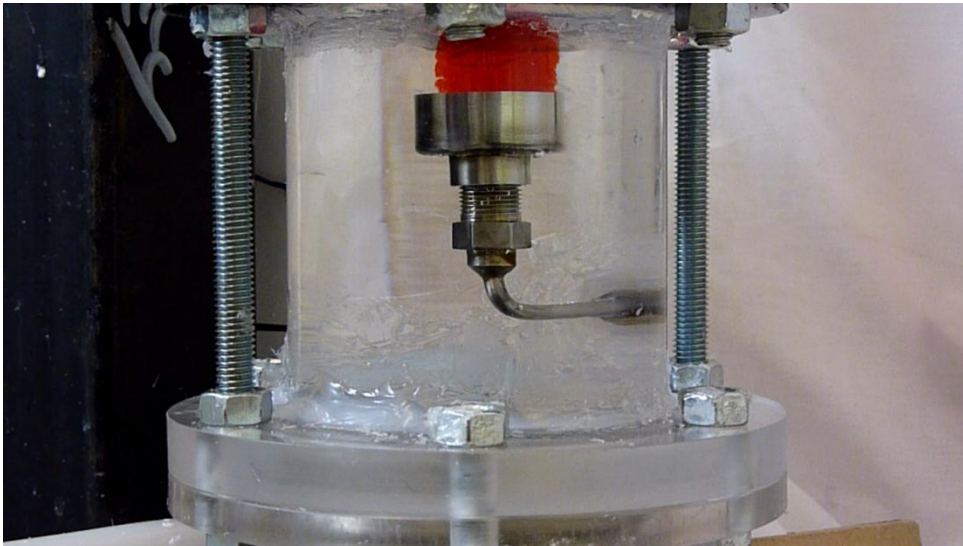
13(a)



13(b)







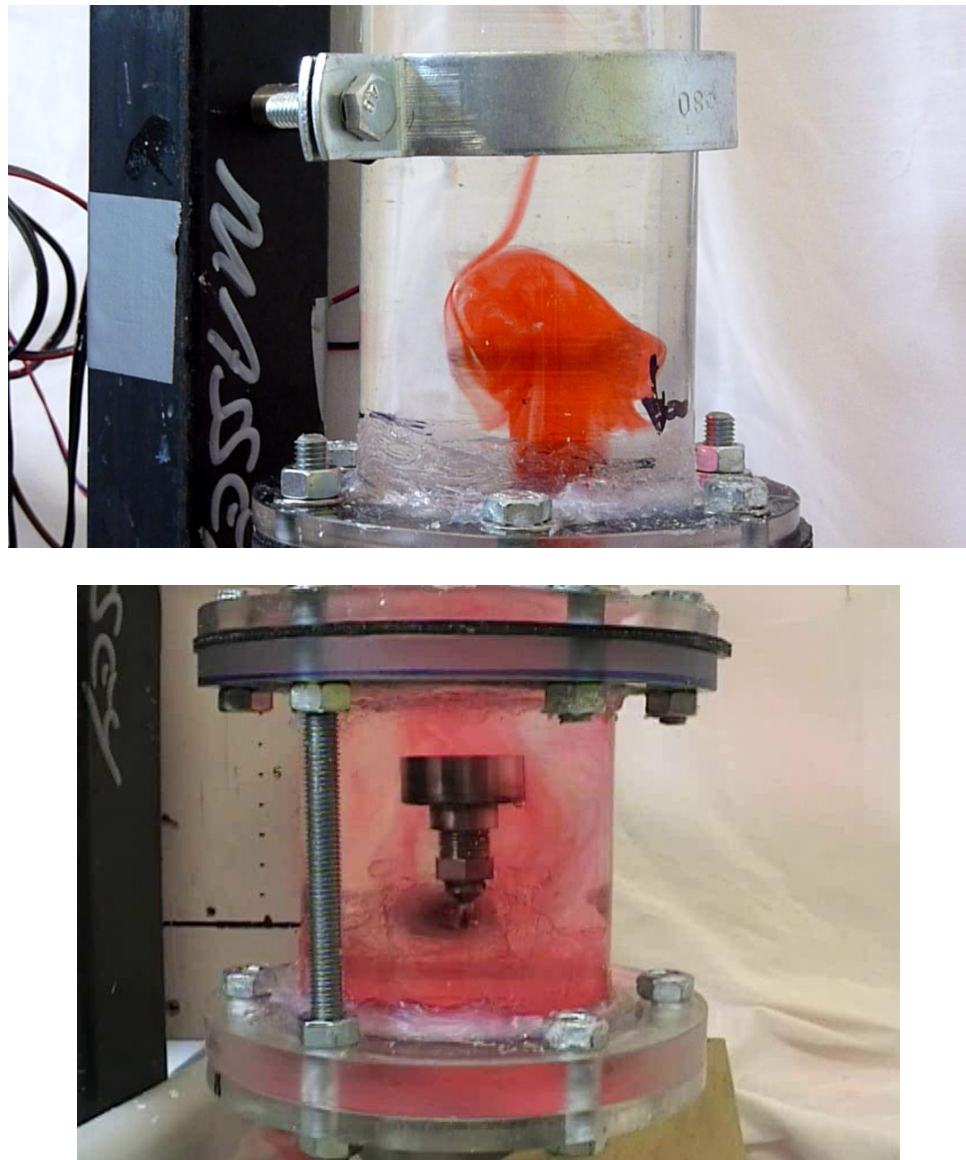
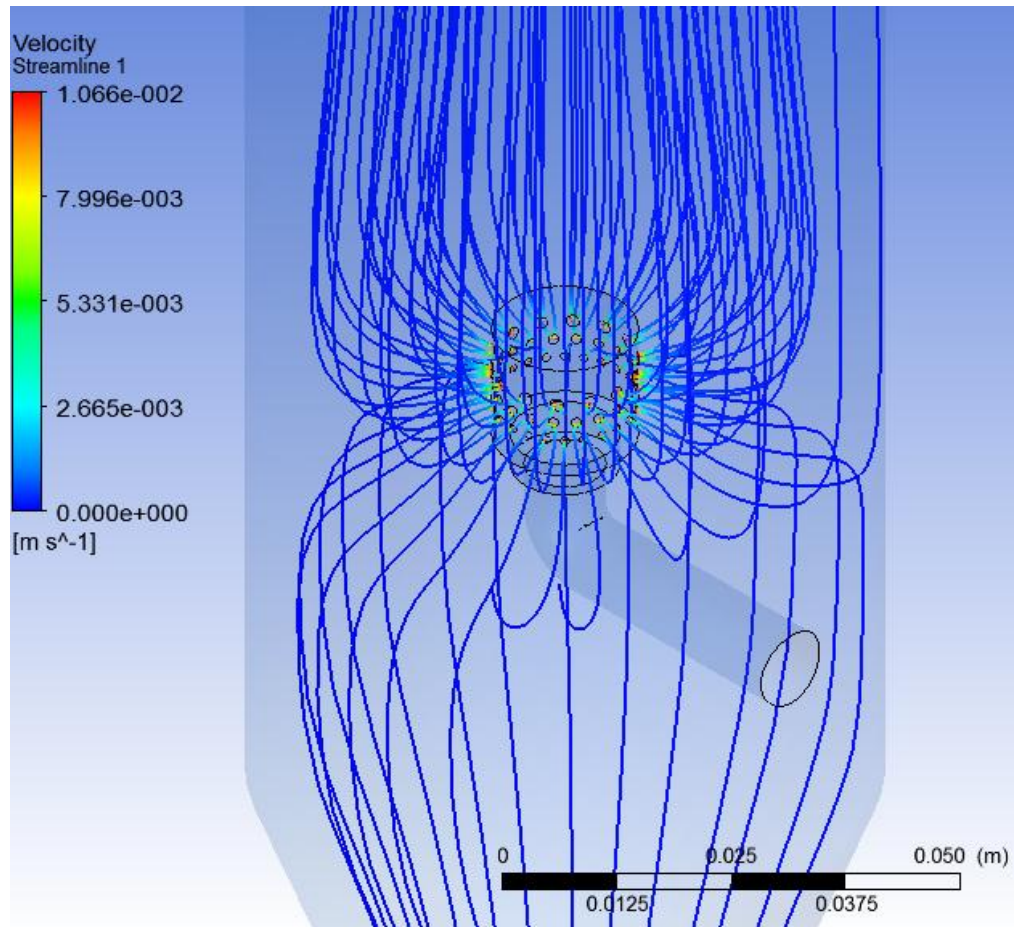


**Figure 4.13** The streamlines of fluid of a vertical column with one pipe upward inlet

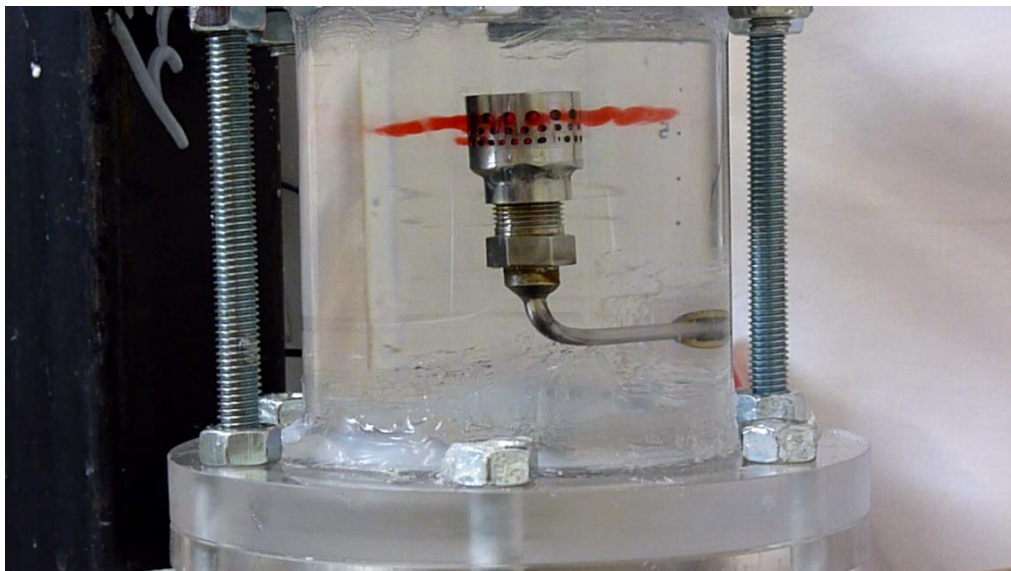
Figure 4.13(a) shows the simulation results of fluid streamlines, which is injected in to the column by the one pipe upward inlet. The fluid will flow up and spread out over the cross section of the column. When the flow is near the wall, some fluid has the lower velocity and flow down to the bottom of the column. It is different from the experimental results as shown in Figure 13(b). Most fluid flows in center of the column zone and flows up to the top. Some dye flows over the injection and goes down before reach the wall of the column. It caused the density and viscosity of dye is more value compared with the water.

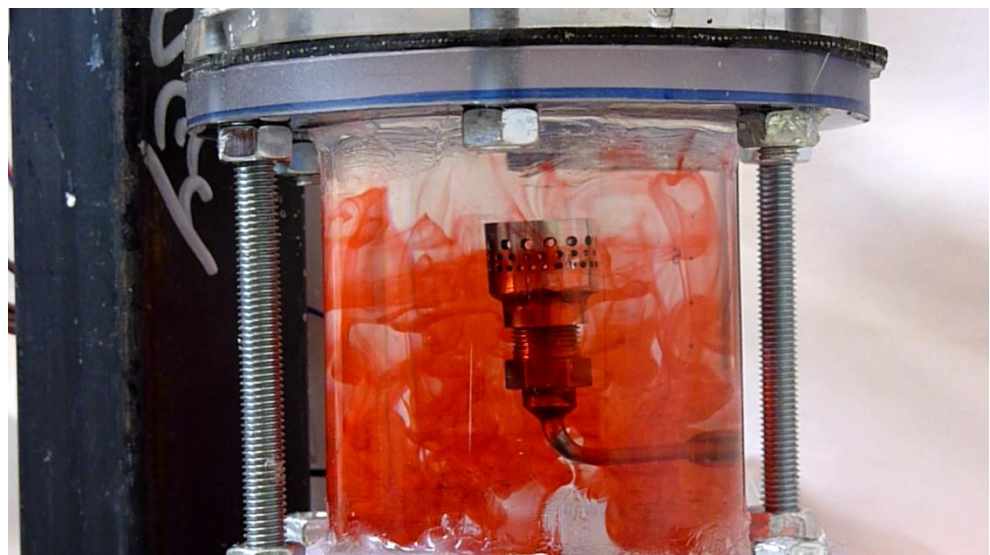
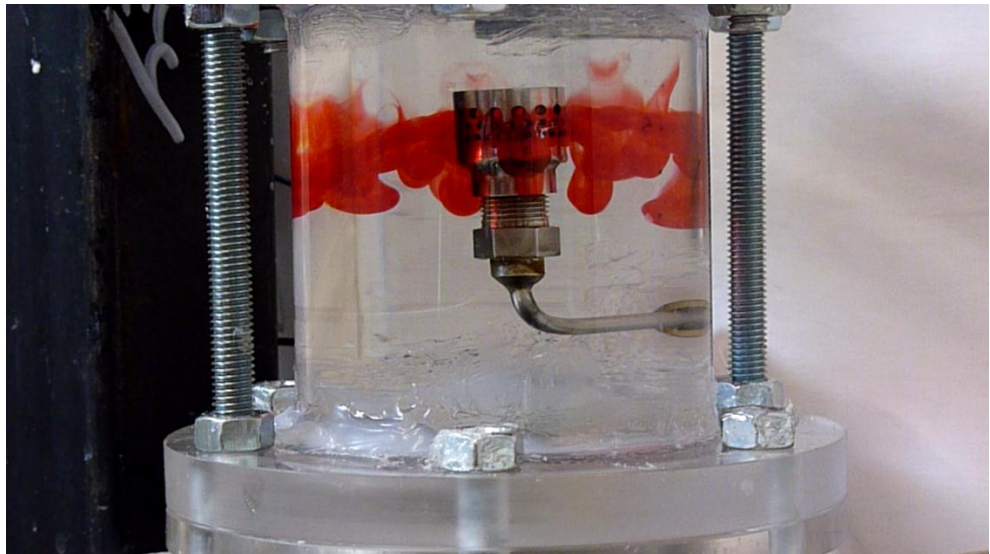
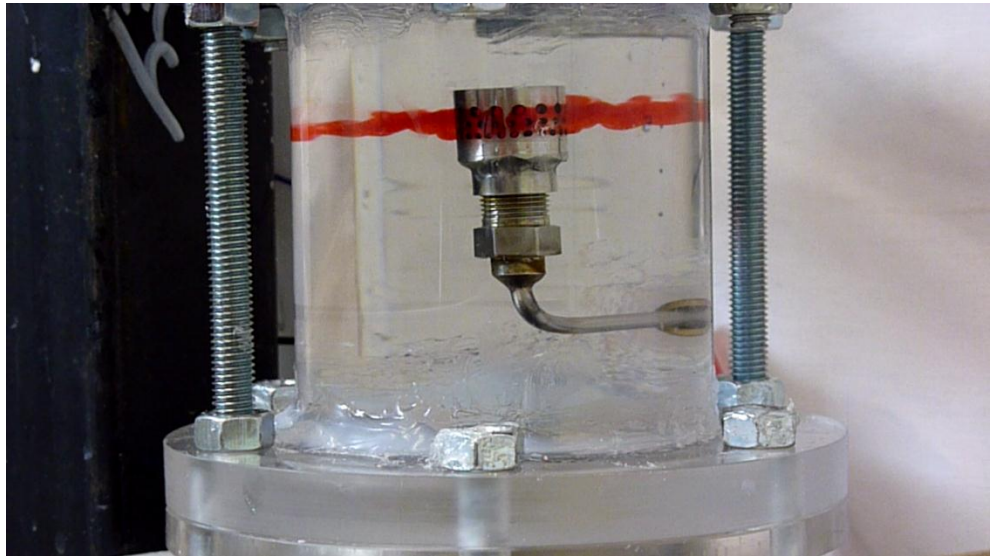


14(a)



14(b)







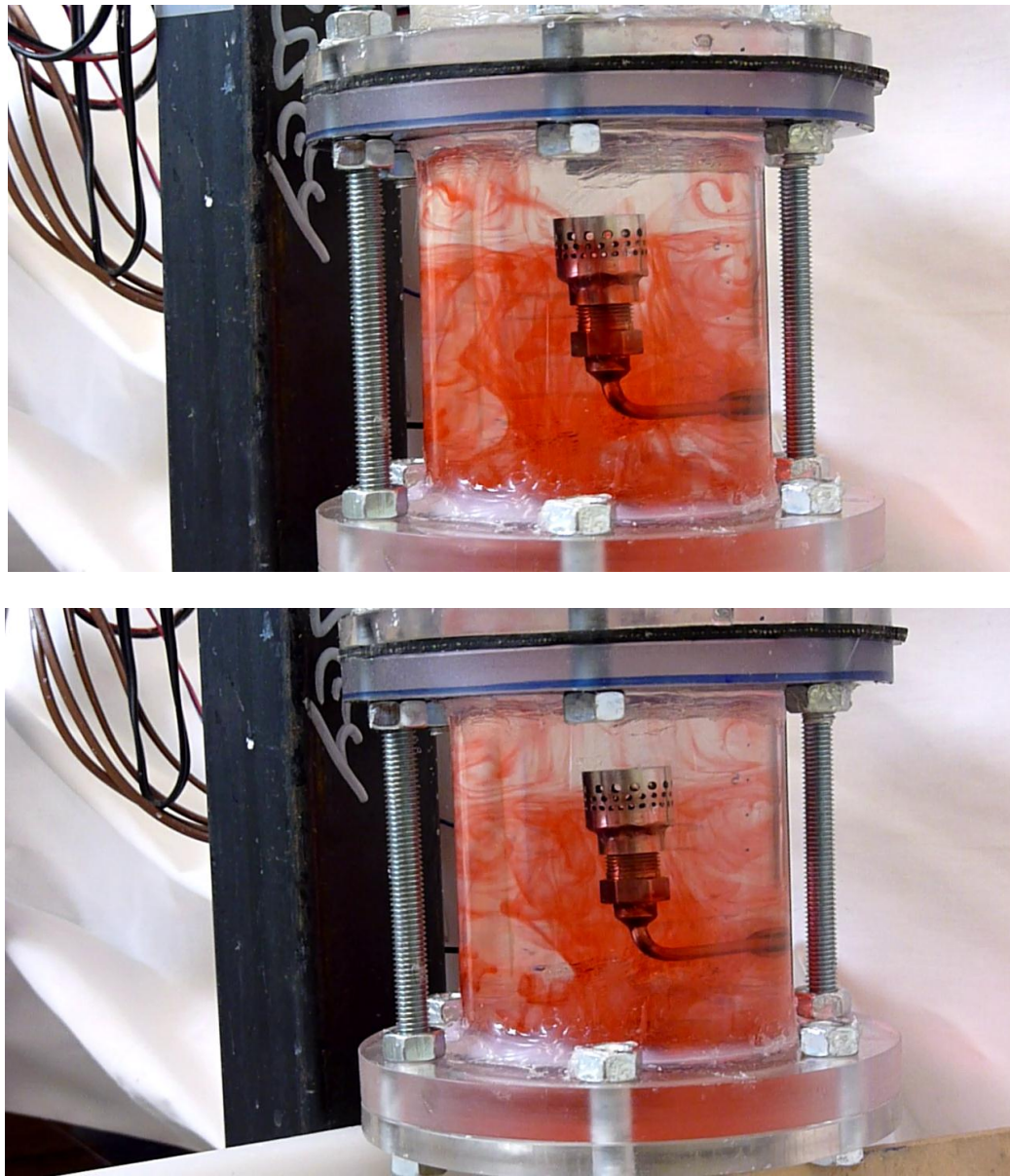


**Figure 4.14** The streamlines of fluid of a vertical column with one pipe sideward inlet

From the simulation, the fluid from the one pipe sideward inlet divided into two directions obviously. Due to the inlet has the hole in the 3 rows which are top, middle and bottom as shown in Appendix A. The fluid that flows from the top and the middle row will flow up to the top of the column while the fluid that flows from the bottom row will flow down to the bottom of the column. When compare to the experimental results found that most dye flow from the one pipe side ward inlet will settling down to the bottom immediately. Some of them are striped to the top by water. Dye will circulate as two circles in the upper and the lower zone of the inlet when the system is steady state.

#### 4.5 New design of pipe inlet

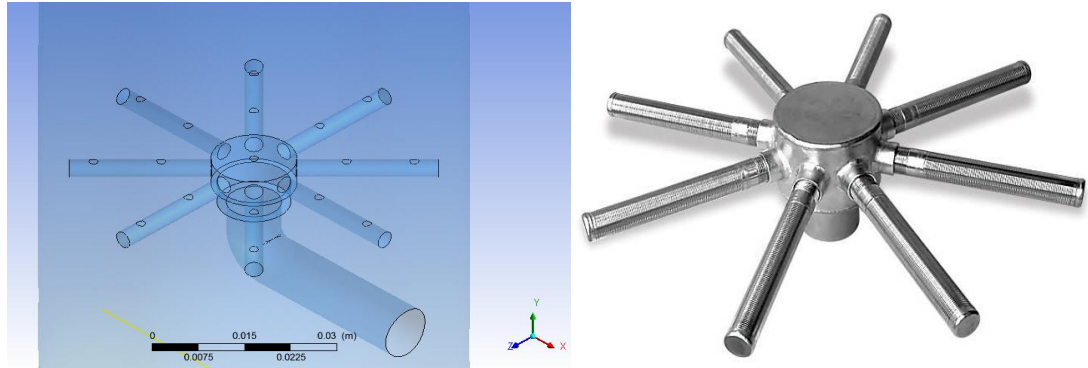


**Figure 4.15** New one pipe inlet

The 16-pipes inlet provides the fully-developed laminar flow fastest because it has better distribution than one pipe inlet. Hence, the new feed inlet is designed based on the distribution of fluid flow from the inlet. Figure 4.15 proposed the picture of new feed inlet in the simulation view and in the actual model. The CFD simulation is used to test an ideal as the following section.

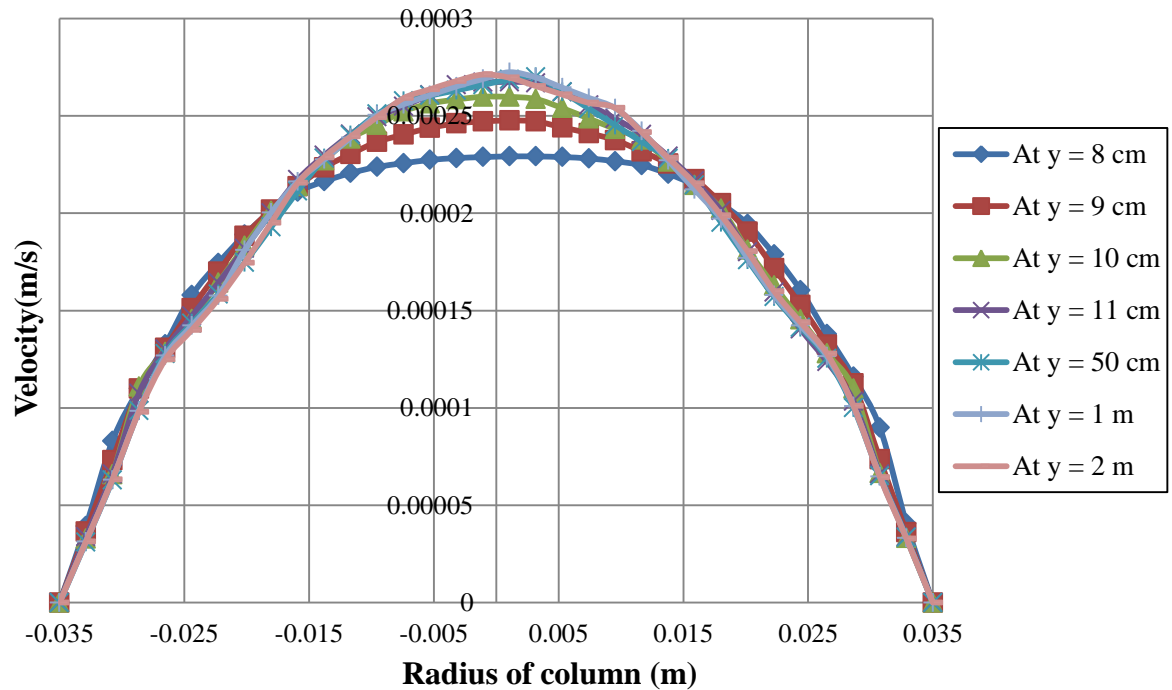


**Figure 4.16** The velocity profiles of fluid at the position near a fully-developed laminar flow



This figure represents velocity profiles at the position near a fully-developed laminar flow of new one pipe inlet. It can observe that the green line locates at 10 cm that is the last position before the fluid reaches the stability and the next one at 11 cm represents a laminar profile. Thus, the fluid in the vertical column with the new one pipe inlet is a fully developed to laminar flow at 11 cm height.

#### 4.5.1 Comparison between the 16-pipes upward inlet and the new one pipe inlet

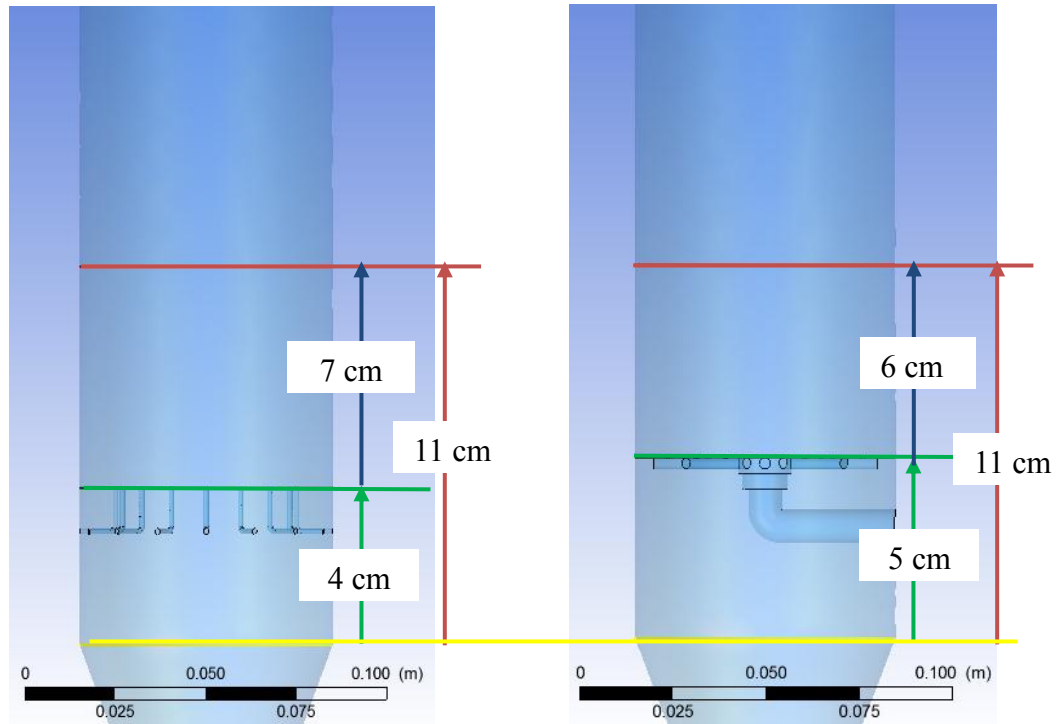


**Figure 4.17** The comparison of heights in which feed inlet designs develop the fully-developed laminar flow

The comparison between 16-pipes upward inlet and new one pipe inlet are shown in this figure. The yellow line represents the reference level which  $y$  equals to zero. The red line shows the height of the fully develop laminar flow measured from the reference level. The green line is the height of the feed inlet compared with the reference level. So, the real height that fluid develops fully laminar flow equal to the height of the red line subtracts the height of the green line as shown in the blue line. It can conclude that the new one pipe inlet provides the fully-developed laminar flow at 6 cm measured from the inlet. Therefore, the new one pipe inlet reaches the stable faster than 16 pipes upward inlet 1 cm.

## **CHAPTER 5 CONCLUSIONS AND RECOMMENDATIONS**

### **5.1 Conclusions**

From the results and discussion, it shows that Computational Fluid Dynamics can be used to study the fluid flow behavior in a vertical column with various feed inlets. The lowest levels of different feed inlet designs used to develop the laminar flow are determined by the simulation results. The level of a fully-developed laminar flow or the level of complete parabolic velocity profile is represented in the previous chapter. The simulation results demonstrate that 16-pipes inlet provides the fully-developed laminar flow fastest at 7 cm measured from the inlet followed by one pipe sideward inlet and one pipe upward inlet at 9.9 and 11.2 cm., respectively. Since 16-pipes inlet gives better distribution than other inlets. Hence, a new one-pipe inlet is designed to improve the distribution of the liquid feed. The simulation result shows the proposed new feed inlet can develop the laminar flow fastest at 6 cm from reference level.

For the experiment, the pathway of fluid from the feed inlet can be clearly observed and was used to compare with streamlines from CFD simulation. It was found that the direction of fluid flow is similar as the design of feed inlet but there are some errors. Due to dye used to observe the fluid flow behavior, the physical properties of dye are different from water such as density, viscosity and diffusivity coefficient.

### **5.2 Suggestions**

1. The appropriate feed inlet for the development of fully laminar flow need to be well distribution along the radius of a vertical column.
2. The physical properties of dye are suitable for selection to do the experiment as following
  - The density( $\rho$ ) and viscosity( $\mu$ ) should be the same of water.
  - The diffusivity coefficient(D) need to be lowest.

### **5.3 Future works**

1. Enable more equations in CFD model such as lactose crystallization to predict the particle formation and energy balance to calculate the temperature of a vertical column.
2. Design the new feed inlets and create the CFD model to prove an ideal without making the real one.

## REFERENCE

1. A. Mersmann, 2001, **Crystallization Technology Handbook 2<sup>nd</sup> edition**. ISBN 0-8247-0528-9 [online], Available: <http://en.wikipedia.org/wiki/Crystallization>, [2011, May 3].
2. K. Liang Jessica, 2003, **Small Molecule Crystallization, Department of Chemical Engineering, Illinois Institute of Technology** [online], Available: <http://acaschool.iit.edu/lectures04/JLiangXtal.pdf>, [2011, May 3].
3. Peter Widas, 1997, **Introduction to Finite Element Analysis, Virginia Tech Material Science and Engineering** [online], Available: <http://www.sv.vt.edu/classes/MSE2094/NoteBook/97ClassProj/num/widas/history.html>, [2011, May 3].
4. Rinil Kuriakose, C. Anandharamakrishnan, 2010. Computational fluid dynamics (CFD) application in spray drying of food products. **Trend in Food Science & Technology** 21, 382-293
5. Dmitri Kuzmin, **Introduction to Computational Fluid Dynamic** [online], Available: <http://www.mathematik.uni-dortmund.de/~kuzmin/cfdintro/lecture1.pdf>, [2011, May 3].
6. He, Yinghe (2009) Uniformity of particles from laminar jet break-up. ISBN 978-0-920804-44-5. **8th World Congress of Chemical Engineering**, 23-27 August, 2009, Montreal, Quebec, Canada.
7. J.S McLeod, A.H.J Paterson, J.E Bronlund, J.R Jones, 2010. Nucleation of Alpha lactose monohydrate induced using flow through a venturi orifice. **Journal of Crystal Growth** 312 (2010). 800–807. School of Engineering and Advanced Technology, Massey University, New Zealand.
8. Gerald Recktenwald, 2002, **Fully-Developed Flow in a Pipe: A CFD Solution** [online], Available: <http://web.cecs.pdx.edu/~gerry/class/ME448/codes/fullyDevelopedPipeFlow.pdf>, [2011, May 3].

## **APPENDIX A**

### **The geometry of Crystallization Column and Feed Inlets**

### A.1 The geometry of crystallization column

Crystallization column has the diameter and the height equal to 7 cm and 3.5 m respectively. It is made from the transparent glass, which can see the fluid inside the column. The inlet of crystallization column locates at the bottom of the column. The part of inlet can be interchangeable to other types of inlet, which has 10 cm length (see Figure A1). There are 3 inlet types that is designed to develop the laminar flow as soon as possible.

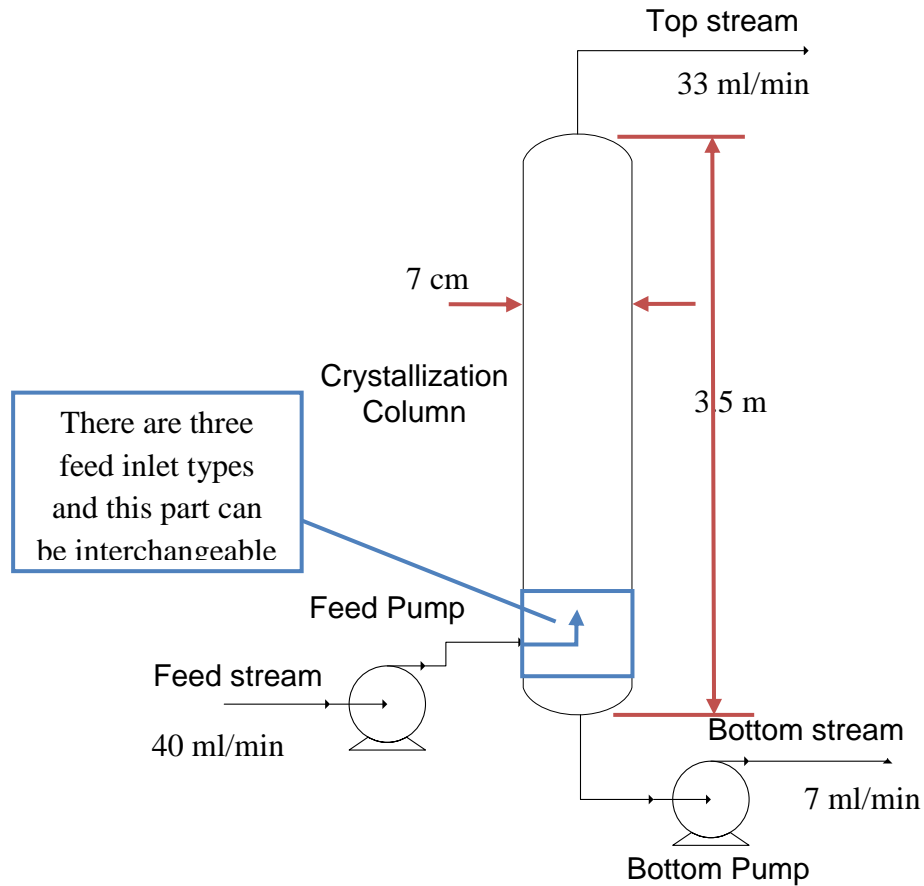


**Figure A.1** The crystallization of the column

As Figure A1, the fluid is pumped into the column through the inlet (injection) with flow rate 40 mL/min and the fluid flow exits at the top and the bottom of the column with flow rate 33 mL/min and 7 mL/min respectively.

### The reference position

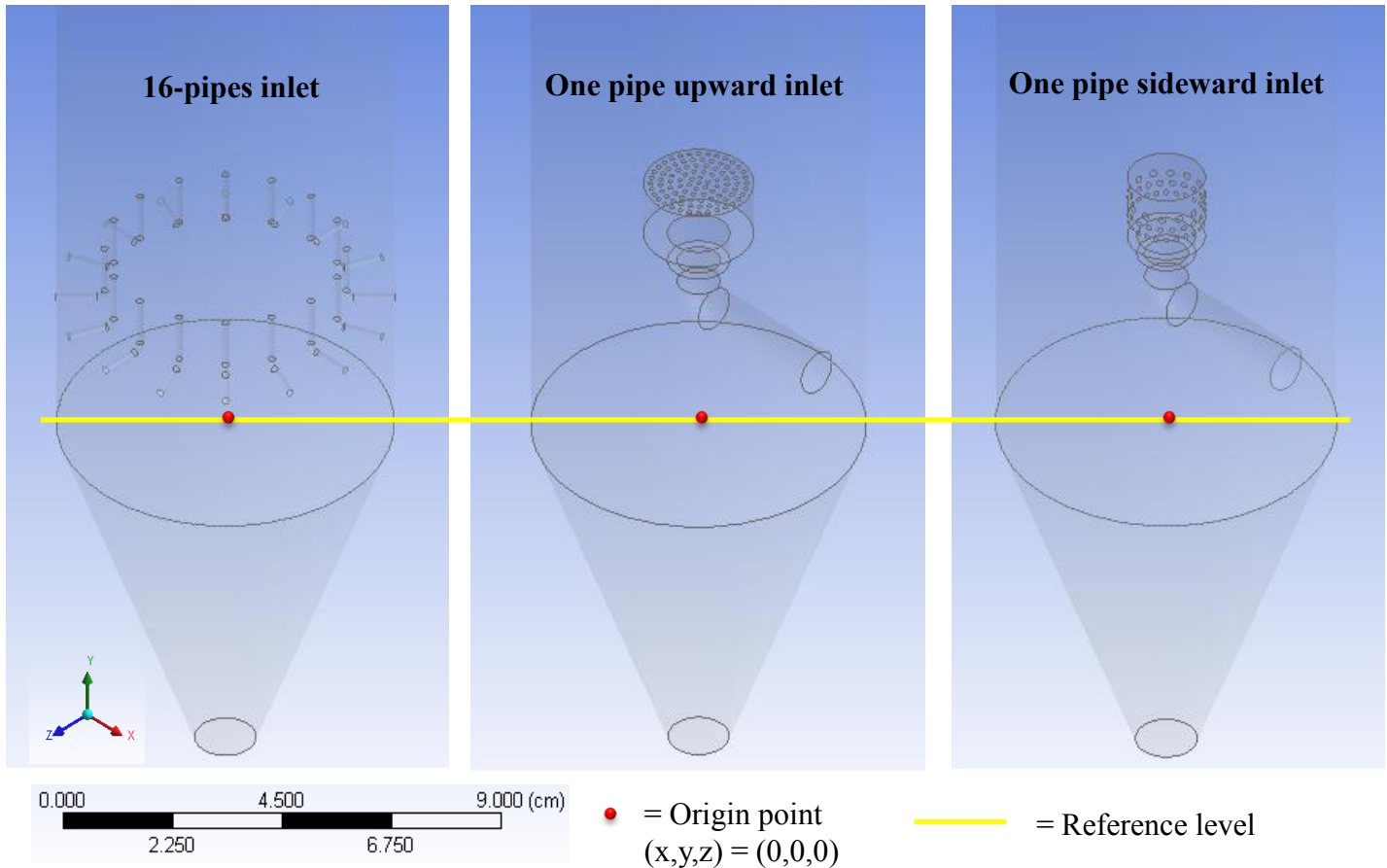


**Figure A.2** The reference level of CFD models

The reference position in which y-axis equals to zero is at the bottom of the column not including a cone shape.

### A.2 The dimensions of feed inlets

Three types of feed inlet are shown as the following. Several color lines shows the dimensions of feed inlets. The red lines represent general lengths of each parts of inlet design while the green lines show the level of feed inlets. The yellow line indicates the reference position.

### 1. 16-pipes inlet

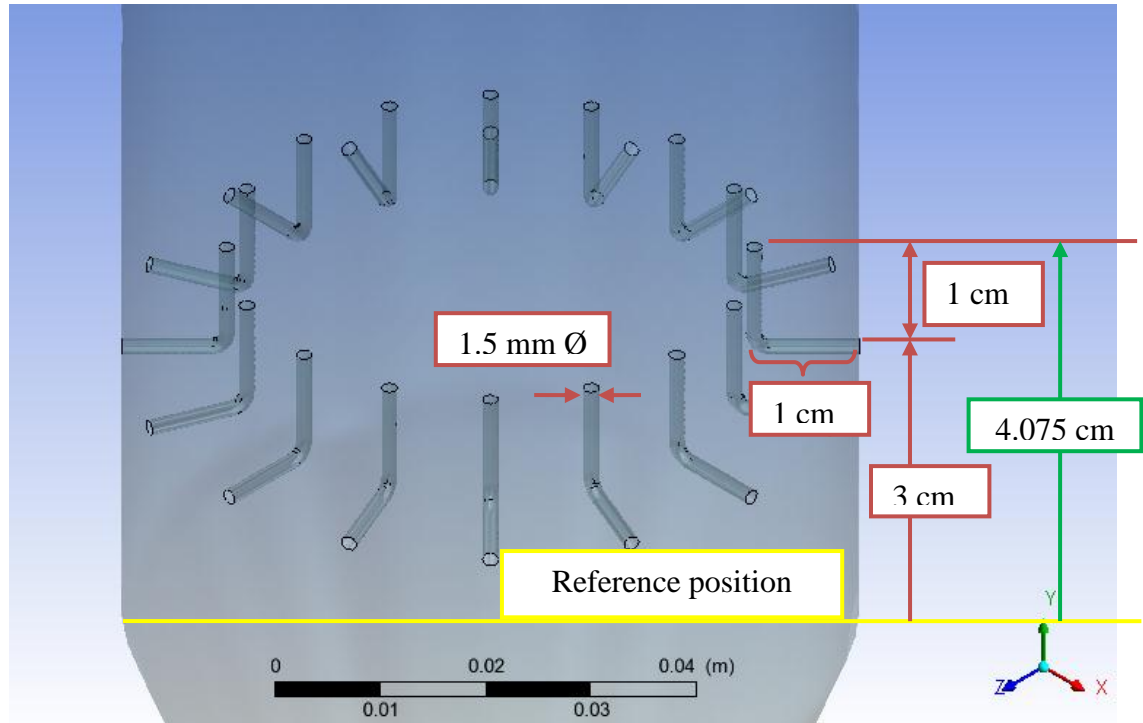


**Figure A.3** The dimensions of 16-pipes inlet type

### 2. One-pipe upward inlet

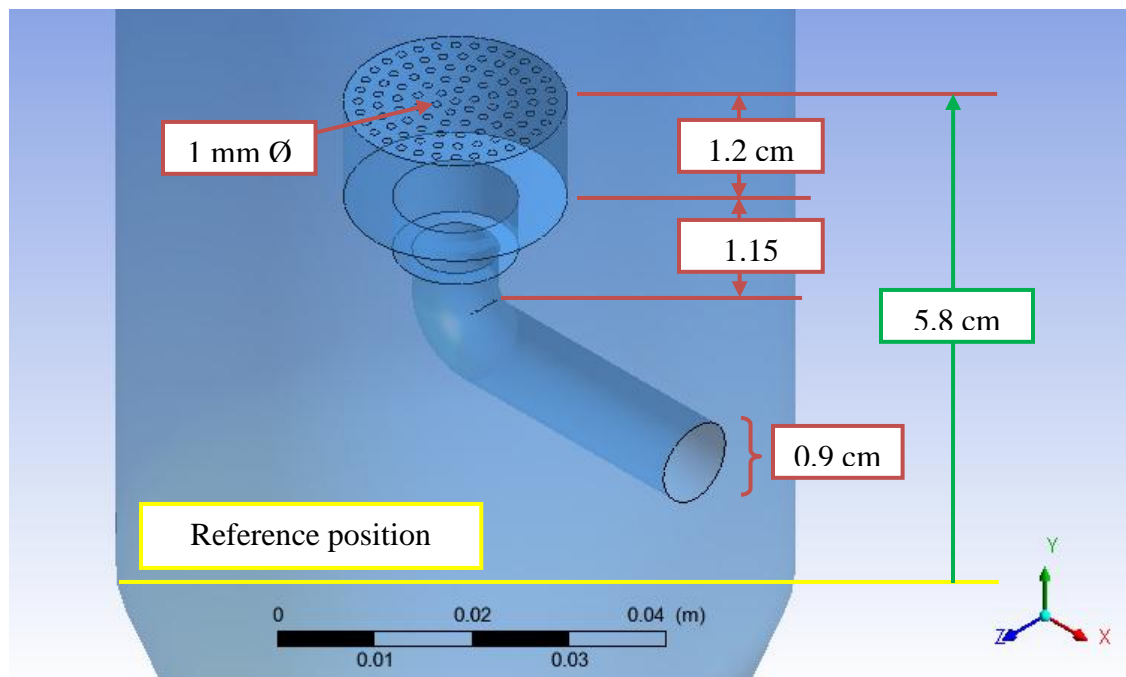


**Figure A.4** The dimensions of one pipe upward inlet type

### 3. One-pipe sideward inlet

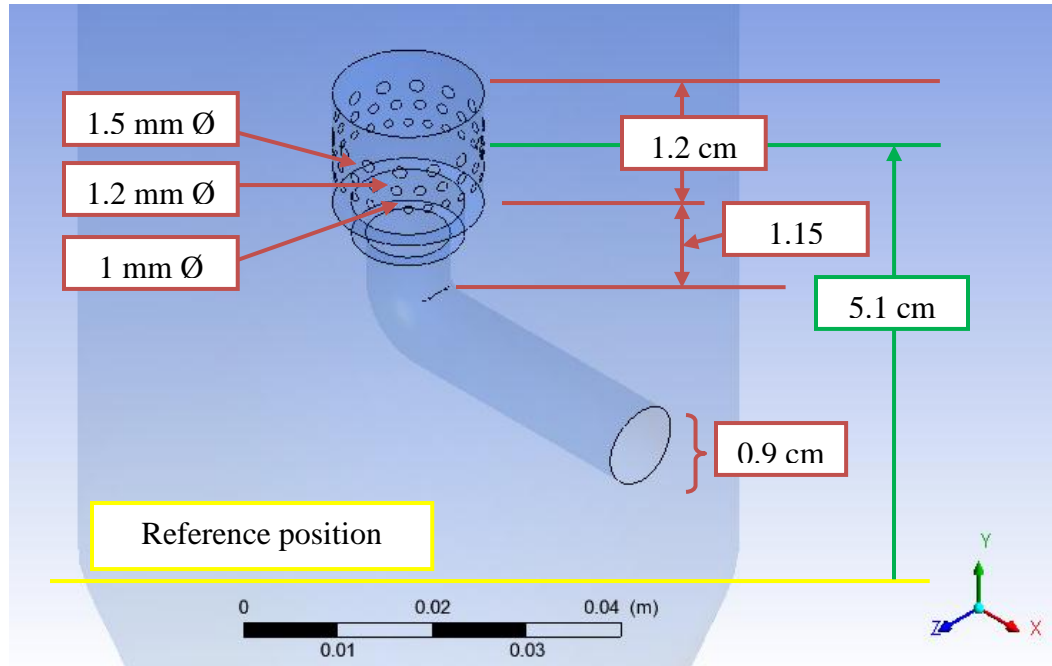


**Figure A.5** The dimensions of one pipe side inlet type

### 4. New one-pipe inlet

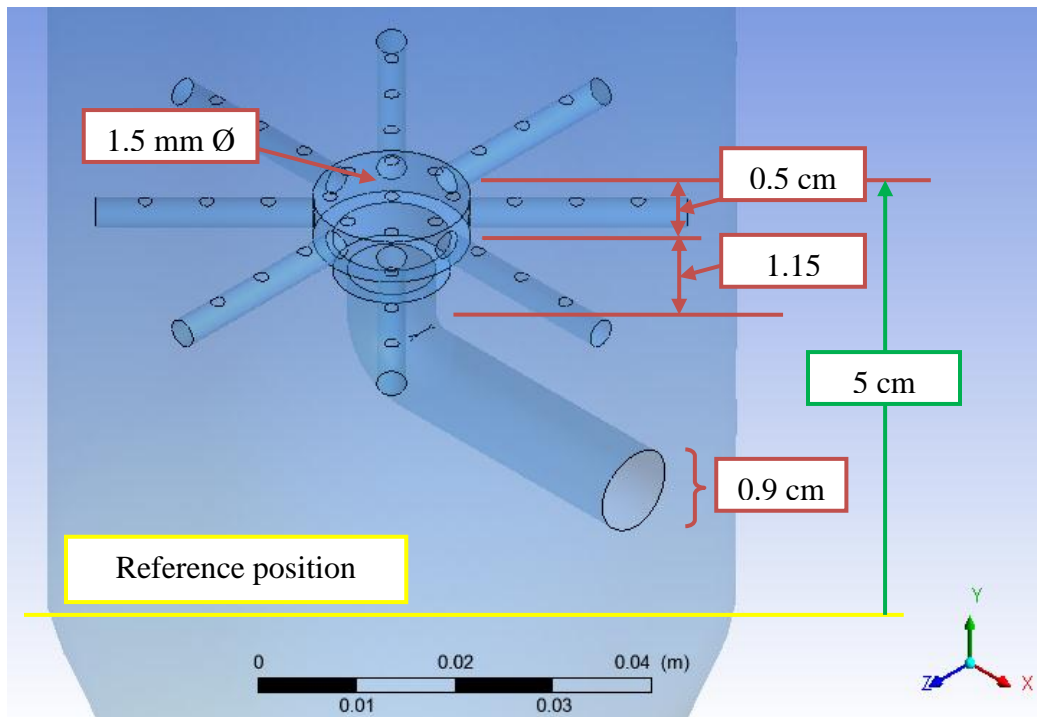


**Figure A.6** The dimensions of one pipe side inlet type



**Appendix B**  
**The physical properties**

**Table B.1** The physical properties of material

<b>Material</b>	<b>Physical properties</b>	
	<b>Density(kg/m<sup>3</sup>)</b>	<b>Viscosity(kg/(miss))</b>
Whey*	1,100	0.0025
Water	997	-
Dye	1,020	-

\* This material is used to simulation.

## **Appendix C**

### **Experimental data**

In order to validate the CFD simulation results, the experiments of three inlet types is set up and water is used in experiments as a feed. Before experiments are performed. A meter stick is built for measuring the height of liquid at varies time. At the steady-state condition, the red dye will be injected into a vertical column to see fluid flow patterns. The steps of experiment consists as the following.

1. Fill the vertical column with water.
2. Calibrate the top and bottom flow rates by using stop watches and graduated cylinders.
3. Inject the red dye into a vertical column with different method of injection.
4. Record the fluid flow by using cameras.

Between step 1 and 2, it should wait a few minutes (2-3 minutes) to allow the flow reached a steady-state before measuring the flow rates. In step 3, there are two different methods of dye injection such as pulse and step injection. A pulse injection is injecting whole dye (0.2ml) in once time while a step injection is injecting solution of dye prepared by mixing dye (0.2ml) and water (2,000ml) in a certain period.

In order to know about some background of dye, A weighing apparatus is used to measure the density of material. The specific volume of samples equals to 1 mL. The density of dye and water are  $1,020 \text{ kg/m}^3$  and  $997 \text{ kg/m}^3$  respectively.

Three inlets used in experiments are 16-pipes inlet, one pipe upward inlet and one pipe sideward inlet. Each inlet has to be done the experiment two times because there have two different injection methods. The experimental results are discussed in following topics.

\* Red color and parenthetical time is the time that is indicated in video camera files.

## 1. 16-pipes inlet

### 1.1 Pulse injection

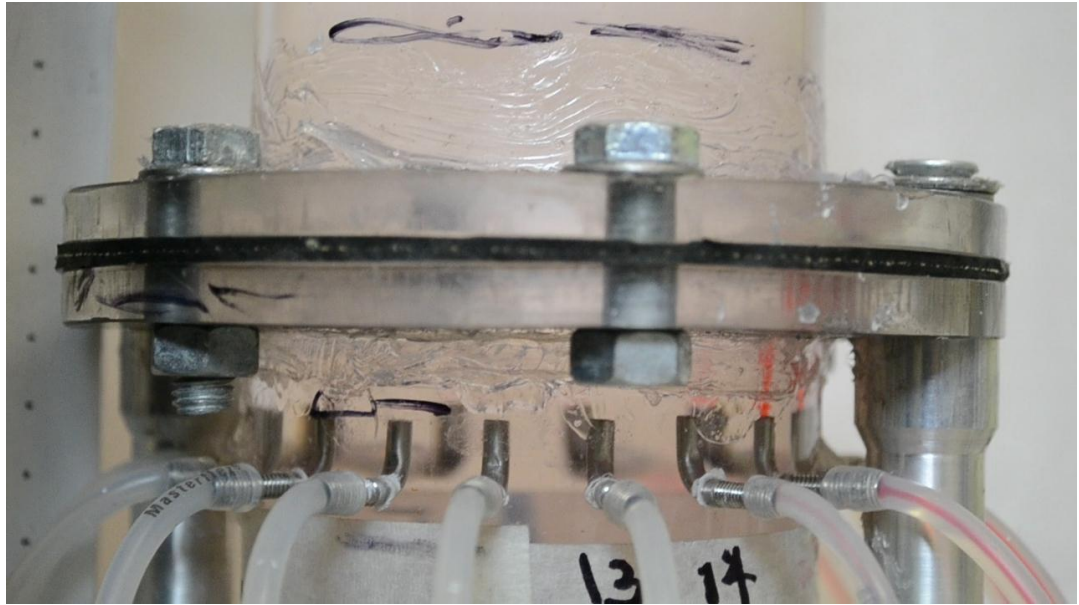


**Figure C.1** 16-pipes inlet at the initial time,  $t = 0$  (16sec dye injected)

This figure is shown the starting point of 16-pipes inlet experiment. A dye are injected to a vertical column by using pulse injection method. It can be observed that dye flows into a column through right pipes before left pipes because the right-hand side pipes is nearer the distributor than left-hand side pipes.



**Figure C.2** 16-pipes inlet at time,  $t = 14$  seconds (30 sec dye injected)

At  $t = 14$  seconds, the streamline of dye is split into two directions. One is going upward along the column. The velocity of another is decrease and then the stream circulates into the center of the column. The average velocity measured by distance and time is about  $3 \times 10^{-3}$  m/s at 12 cm height of the column.

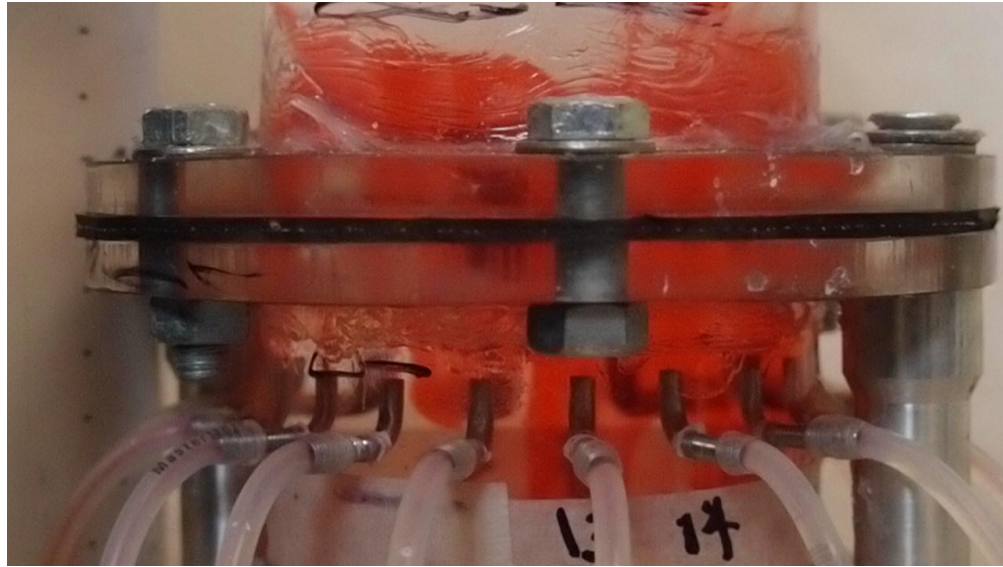


**Figure C.3** 16-pipes inlet at time,  $t = 34$  seconds (50 sec dye injected)

Figure C.3 is also shown that dye circulates to the center of the column and most of dye is settling to the bottom. Since dye has the higher density than water. In addition, dye still flow in the left pipes but a red color of dye in the right pipes are fading as described in Figure C.1.



**Figure C.4** 16-pipes inlet at time,  $t = 5$  minutes 22 seconds (6mins 29sec dye injected)

At 23 cm height, the velocity of dye is approximately  $7.4 \times 10^{-4}$  m/s. Dye congregates close to one side of the wall as a balloon shape and floats up to the top slowly as shown in the Figure C.5.



**Figure C.5** 16-pipes inlet at time,  $t = 4$  minutes 58 seconds (7mins 5sec dye injected)

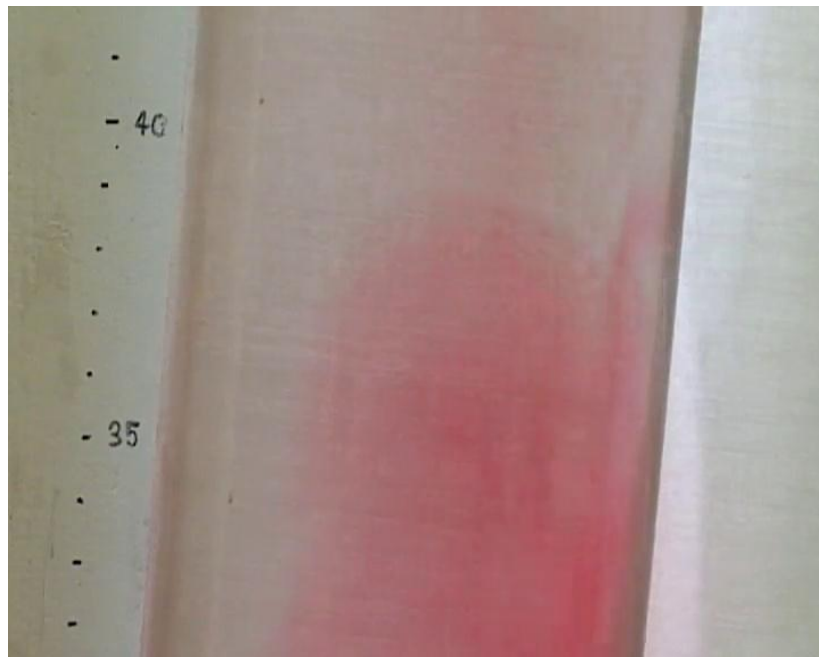


**Figure C.6** 16-pipes inlet at 39 cm height

As figure 6, it can be observed a parabolic velocity profile at 39 cm height and the velocity of dye is  $1 \times 10^{-3}$  m/s.



## 2. One pipe upward

### 2.1 Pulse injection

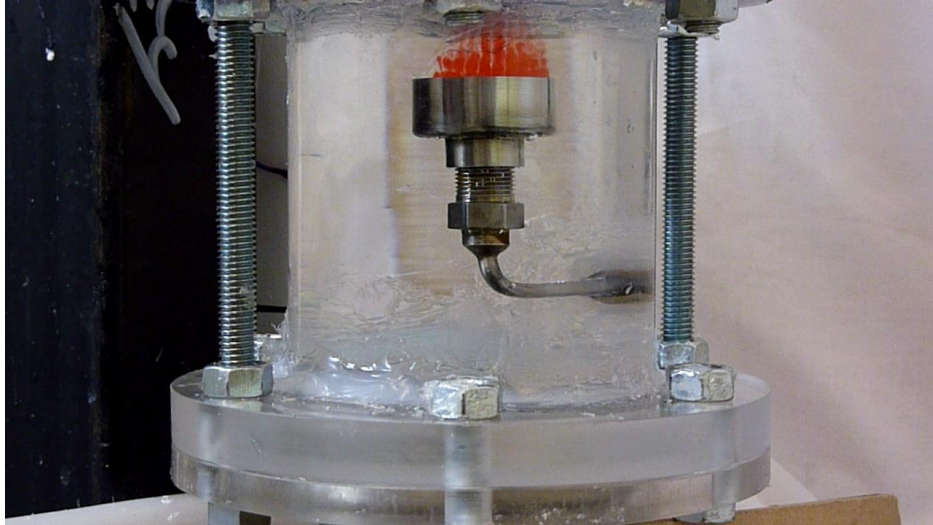


**Figure C.7** One pipe upward inlet near the initial time of injection (31sec dye injected)

This figure shows dye injecting from the nozzle. It can be observed that the velocity of dye is highest at the center of inlet and decrease along with radius. The velocity of dye is about  $1.4 \times 10^{-2}$  m/s.

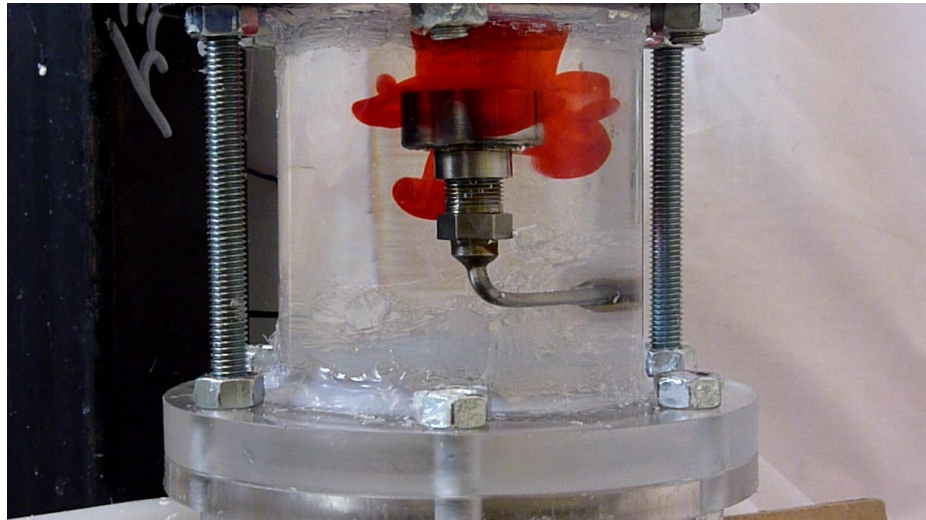


**Figure C.8** One pipe upward inlet at the time,  $t = 14$  seconds (45sec dye injected)

After 14 seconds of dye injection, dye is settling down on side of a nozzle to the bottom. It is a result of dye weight which is more than the water. Including, the velocity of inlet is small to carry dye up to the top.



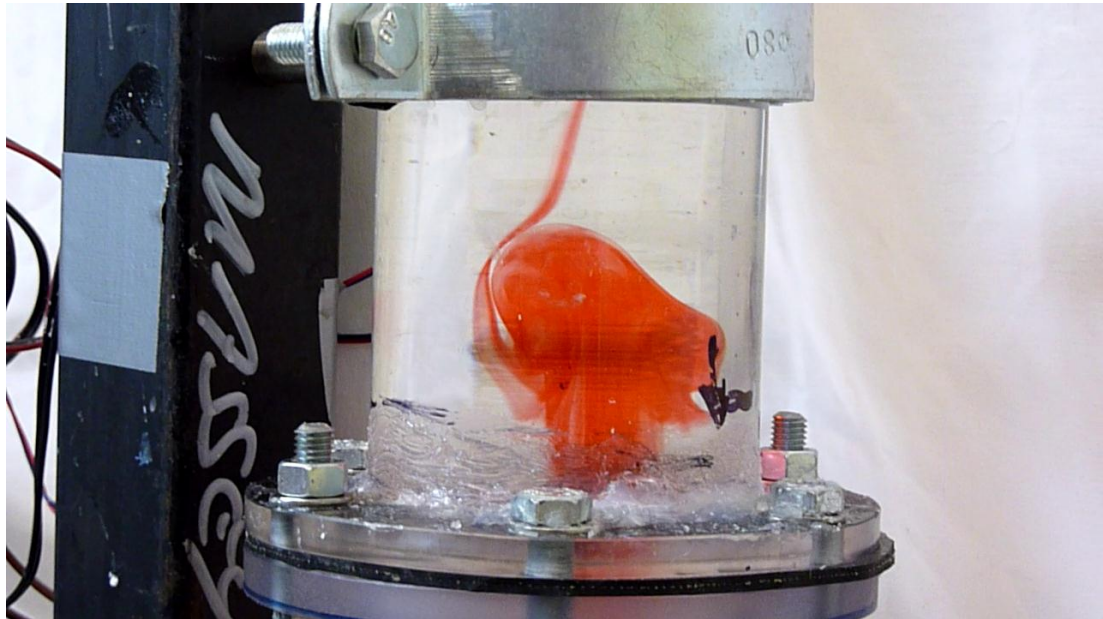


**Figure C.9** One pipe upward inlet at the time,  $t = 43$  seconds (1min14sec dye injected)

As the Figure C.9, there is a group of dye at 15 cm height at 43 seconds after injection.



**Figure C.10** One pipe upward inlet at the time,  $t = 1$  minutes 30 seconds (2min dye injected)

The streamline of fluid flow can be observed at 24 cm height estimated after 90 seconds of injection. The velocity of dye is around  $1.3 \times 10^{-3}$  m/s.

## 2.2 Step injection

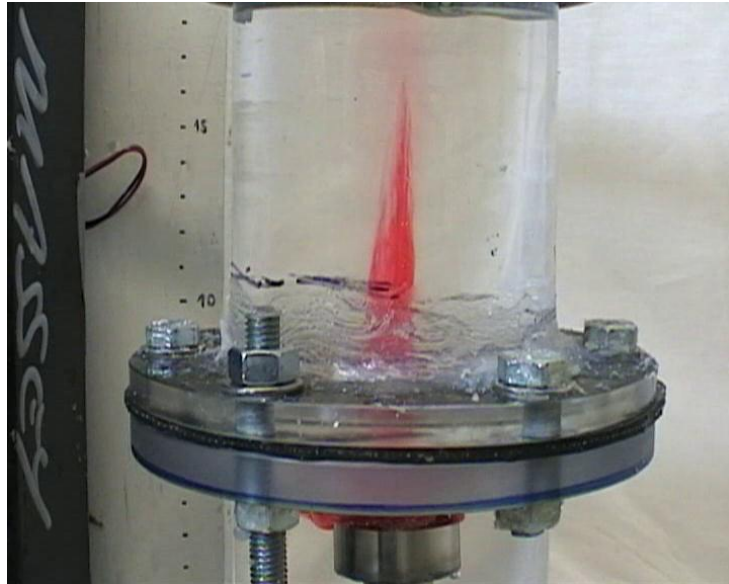


**Figure C.11** One pipe upward inlet at the time,  $t = 14$  seconds (42sec dye injected)

When the pulse injection of one pipe upward experiment is performed, the solution of dye is switched to a new feed in step injection method. As the Fig.11, the velocity of dye can be calculated which is about  $1 \times 10^{-2}$  m/s at 15 cm height.

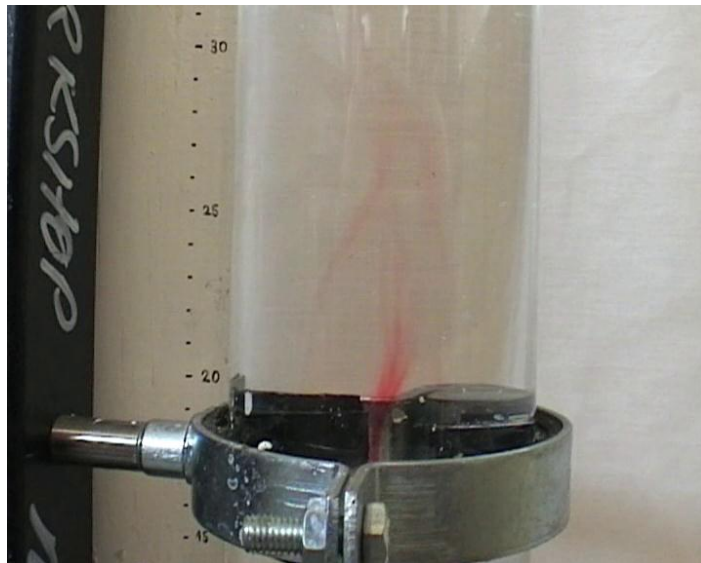


**Figure C.12** One pipe upward inlet at the time,  $t = 28$  seconds (58sec dye injected)

According to Figure C.12, the height of dye at 28 seconds after injection equals 23cm. The velocity of dye is approximately  $3 \times 10^{-3}$  m/s.



**Figure C.13** One pipe upward inlet at the time,  $t = 1$  minutes 50 seconds (2min 17sec dye injected)

It is hard to see the color of dye above the inlet after this time (about 2 minutes) as shown in the Fig 13. The velocity of dye is about  $2 \times 10^{-3}$  m/s.

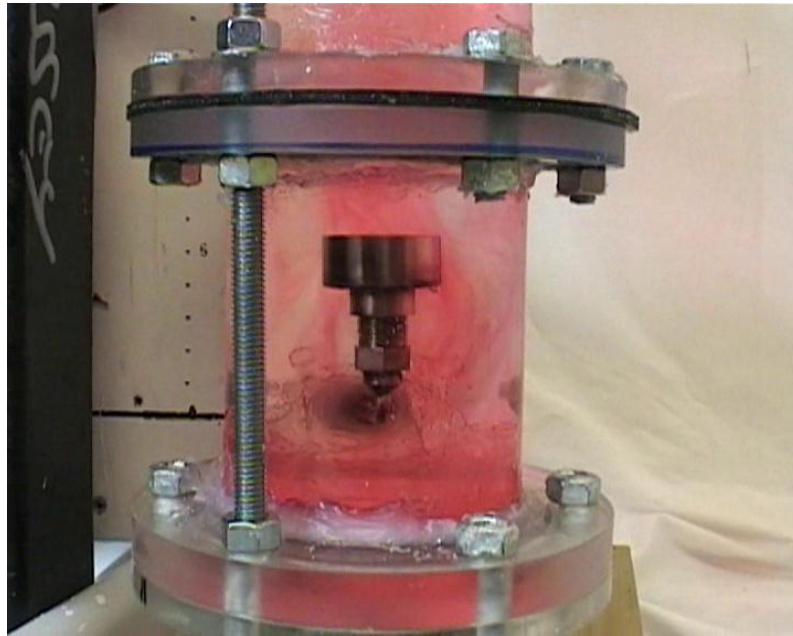


**Figure C.14** One pipe upward inlet at the time,  $t = 5$ minutes 20 seconds (5min 47sec dye injected)

This figure shown the solution of dye is filled in a region of the inlet over a long time (5 minutes after injection).



### 3. One pipe sideward

#### 3.1 Pulse injection

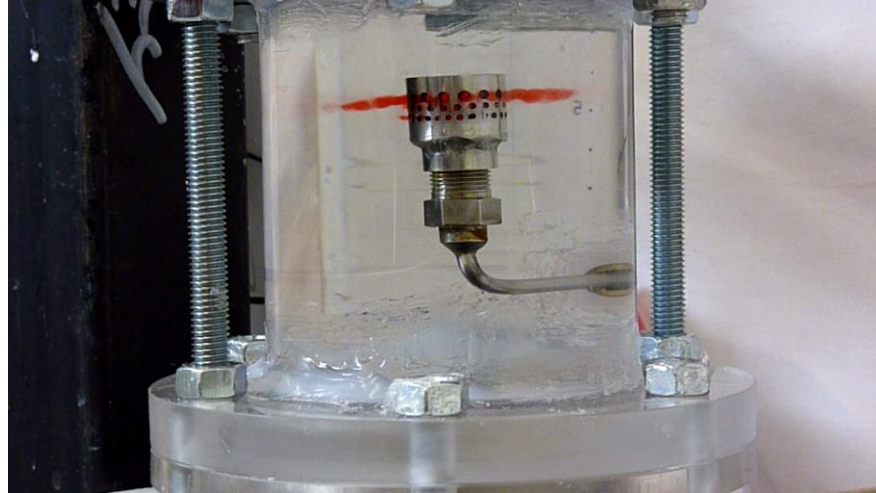


**Figure C.15** One pipe sideward inlet near the initial time of injection (39sec dye injected)

Form the observation, most of dye exit at the highest opening hole of the inlet and have a direction rushing to the wall. Since, dye is pumped into the column with only one pipe inlet and has a high velocity compared with 16-pipes inlet case. It causes the collision between the fluid and the top wall inside the nozzle before coming out of the opening hole on the side wall as the Figure C.15.

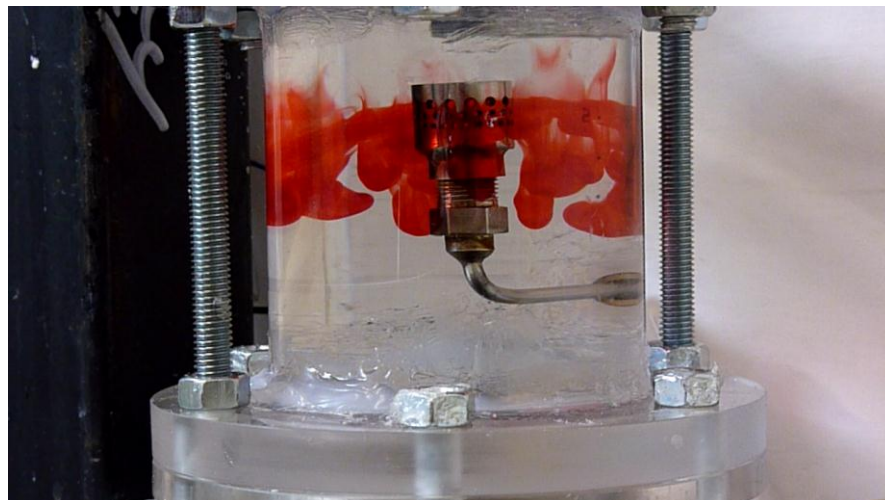


**Figure C.16** One pipe sideward inlet at the time,  $t = 10$  seconds (50sec dye injected)

Over time 10 seconds, a majority of dye have hit the wall and goes downward to the bottom while a minority of dye is stripped by water back to the top.

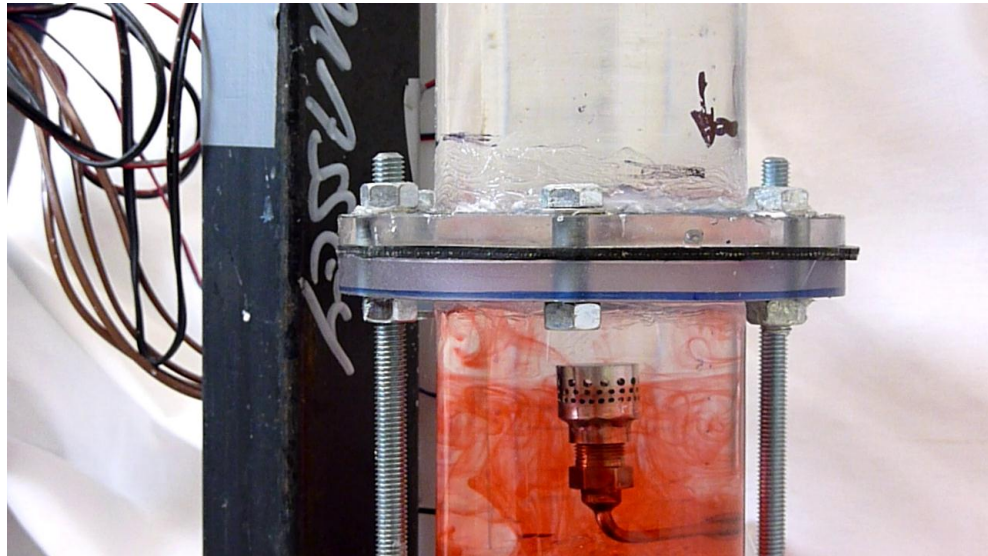


**Figure C.17** One pipe sideward inlet at the time,  $t = 67$  seconds (1min 46sec dye injected)

As Figure C.17, the streamlines of fluid near the inlet can be clearly observed at 67 seconds after injection. In addition, there are two recirculating of fluid. One is above a nozzle. Another one has a bigger radius of cycle and locates at the same level or lower than the nozzle.

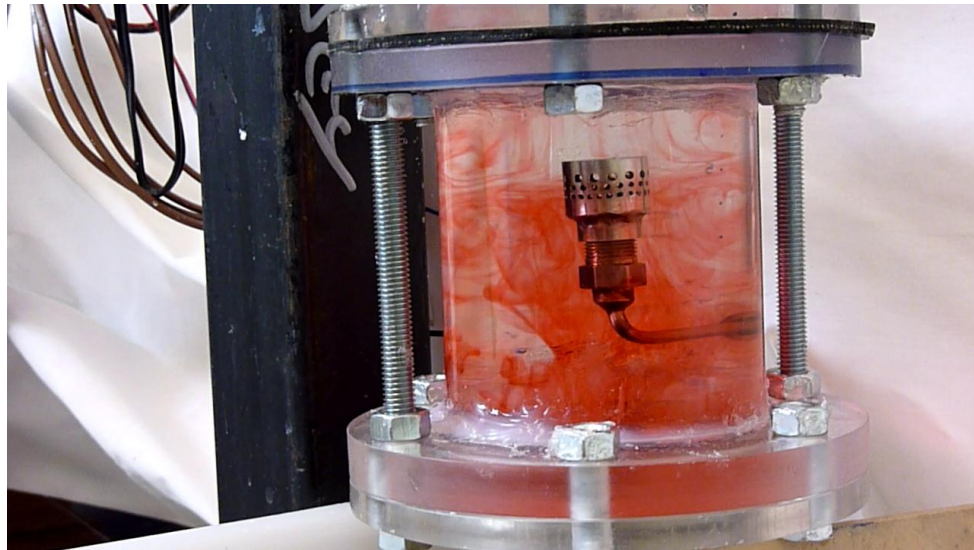


**Figure C.18** One pipe sideward inlet at the time,  $t = 1$  minute 30 seconds (2min 10sec dye injected)

After one and a half minutes, the streamline of dye is also observed but the level of dye does not increase. Since, this injection is only once time injection(pulse). The most of dye circulate at the bottom of the column so it exits with the bottom flow and is not added from the outside.

### 3.2 Stream injection

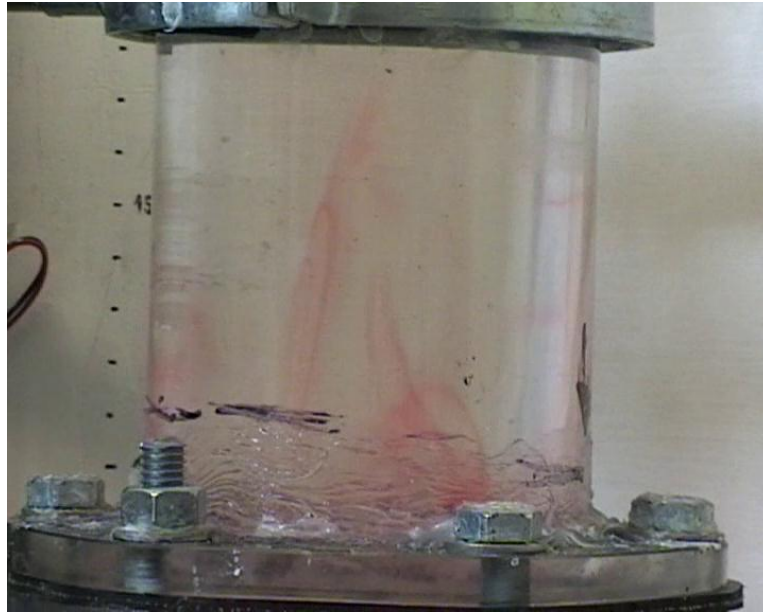


**Figure C.19** One pipe sideward inlet at the time,  $t = 1$  minute 30 seconds (11min 4sec dye injected)

When the injection method is switched to step change, The red color can be observed above the nozzle along the column. So, the velocity of fluid in column can be measured and is about  $1.2 \times 10^{-3}$  m/s at 15 cm height of the column.



**Figure C.20** One pipe sideward inlet at the time,  $t = 3$  minutes 40 seconds (12min 47sec dye injected)

However, the color of dye is fading because this injection is a step injection method and uses a solution of dye by mixing with water. Thus, the solution is diluted throughout the distance it flows. The velocity of dye is around  $7.7 \times 10^{-4}$  m/s at 25 cm height.



**Figure C.21** One pipe sideward inlet at the time,  $t = 6$  minutes 52 seconds (15min 58sec dye injected)

In this figure, the solution will be diluted over the time and gathers at the wall.

### Conclusion

1. From experiments of three inlets, the streamline of fluid can be observed at the region of inlet that are able to validate with CFD simulation results.
2. The velocity of dye can be calculated by using the measurement of distance and time that are collected in following table.

**Table C.1** represents the velocity of dye in each nozzles at different levels of height

Injection	Velocity (m/s)			
	Inlet	10-15 cm Height	20-25 cm Height	35-40 cm Height
16 pipes inlet	$1 \times 10^{-2}$	$3 \times 10^{-3}$	$7.4 \times 10^{-4}$	$1 \times 10^{-3}$
One pipe upward inlet	$1.4 \times 10^{-2}$	$1 \times 10^{-2}$	$3 \times 10^{-3}$	$2 \times 10^{-3}$
One pipe sideward inlet	-	$1.2 \times 10^{-3}$	$7.7 \times 10^{-4}$	-

**Suggestions**

Use another dye which have the physical properties as the following.

- Density,  $\rho$ : similar or near water in order to decrease settlings down due to density different
- Viscosity,  $\mu$ : higher is better because dye can be stripped by water easiler. It results that dye will be the same velocity as water.
- Diffusion Coefficient,  $D$ : The lower diffusion coefficient can reduce the phenomena of mixing between the water and dye. Therefore, the color of dye will be observed gather distance.



## **CURRICULUM VITAE**

**NAME** Mr. Poochet Horkanya

**DATE OF BIRTH** 10 November 1989

### **EDUCATIONAL RECORD**

**HIGH SCHOOL** High School Graduation  
Wat Suthiwaram School, 2003

**BACHELOR'S DEGREE** Bachelor of Engineering (Chemical Engineering)  
Chulalongkorn University, 2009

**MASTER'S DEGREE** Master of Engineering (Chemical Engineering)  
King Mongkut's University of Technology Thonburi, 2011